Chemical Engineering Science 130 (2015) 151–171

Contents lists available at ScienceDirect

Chemical Engineering Science

journal homepage: www.elsevier.com/locate/ces

Exergy efficiency of plant photosynthesis

Cory S. Silva [a], Warren D. Seider [a], Noam Lior [b,*]

[a] Department of Chemical and Biomolecular Engineering, University of Pennsylvania, Philadelphia, PA 19104-6393, USA
[b] Department of Mechanical Engineering and Applied Mechanics, University of Pennsylvania, Philadelphia, PA 19104-6393, USA

HIGHLIGHTS

- We analyze the exergy and energy efficiency of photosynthesis.
- The analysis reconciles the current efficiency predictions that are from 2.6% to 41%, to 3.9%.
- Written in a way to improve the bridge of understanding between biologists and thermodynamicists.

ARTICLE INFO

Article history:
Received 6 October 2014
Received in revised form
17 January 2015
Accepted 14 February 2015
Available online 26 February 2015

Keywords:
Photosynthesis
Carbon dioxide
Thermodynamics
Exergy
Solar energy
Bio-energy

ABSTRACT

With recent concerns about sustainability and environmental protection, growing attention has been focused on biological sources for both chemicals and fuels; however, to analyze such bioprocesses for commercial viability, and to investigate possible efficiency improvements, the theoretical efficiencies must be known as an upper-bound on performance. Since almost all exergy contained in biomass originates from solar radiation, photosynthesis is the gateway to sustainable bioprocess development. The literature shows a wide range of efficiency predictions, 2.6–41%, due to different definitions and methods of analysis. Therefore, the objective of this study is to dissect the complex bio-processes involved in photosynthesis and analyze the exergy flows through the system, analyzing photosynthesis so as to be understandable by both biologists and thermodynamicists. The initial absorption of light has the lowest exergy efficiency, and it accounts for over 64% of the exergy lost throughout the system. For the light reactions, reduction potentials are used to analyze the flow of excited, high-energy electrons through photosystems II and I, resulting in an exergy efficiency for the light reactions of 32 percent. For the dark reactions, the chemical exergy method proposed by Lems et al. (2007) is appropriate. The resulting efficiency of the dark reactions is 81 percent. Exergy losses to transpiration and photorespiration are taken into account, although their effects are relatively small. The overall exergy efficiency of photosynthesis is calculated to be 3.9 percent. The efficiencies of the sub-processes, as well as the overall efficiency, show good agreement with recent publications. Ultimately, the largest losses are due to poor absorption of light and the inefficient electron transfer through the photosystems.

1. Introduction

The flow of solar radiation into the earth's upper-atmosphere is approximately 174,000 TW, of which, 114,000 TW reaches the Earth's surface (Szargut, 2005). That radiation can be converted directly to electricity using photovoltaic devices or indirectly by first converting it to biomass (using photosynthesis) and then combusting the biomass, generating heat for thermo-electric power plants.[1] Other indirect methods of converting solar radiation into electricity use the wind, ocean currents, and ocean temperature differences. Alternatively, photosynthesis can be used to produce energy-dense oils, which are then converted to transportation fuels (Biswas et al., 2013; Dunlop et al., 2013; Silva et al., 2014).

Even more significant than being a source for heat, biofuels, and electricity, biomass is used for the growth of autotrophic

Abbreviations: ADP, adenosine diphosphate; ATP, adenosine triphosphate; CC, Calvin cycle; Ctyb, cytochrome b6f; ETC, electron-transport chain; GAl3P, glyceraldehyde-3-phosphate; G6P, glucose-6-phosphate; $NADP^+$, nicotinamide adenine dinucleotide phosphate (oxidized); NADPH, nicotinamide adenine dinucleotide phosphate (reduced); NAABB, National Alliance for Biofuels and Bioproducts; PAR, photo-active region; PGA, 3-phosphoglycerate; PSI, photosystem I; PSII, photosystem II; P_i, phosphoric acid; PC, plastocyanin; PO, photosynthetic organism; PMF, proton-motive force; RuBP, ribulose-1,5-bisphosphate; RuBisCO, ribulose-1,5-bisphosphate

* Corresponding author. Tel: +1 215 898 4803.
E-mail address: lior@seas.upenn.edu (N. Lior).

http://dx.doi.org/10.1016/j.ces.2015.02.011
0009-2509/

[1] Fossil fuels most likely originate from photosynthetically produced biomass (plankton and plants) from the distant past.

organisms, such as plants. Autotrophic organisms are complex chemical machines that serve as food and building materials for humans and animals, and they also have a vital impact on the earth's ecology and climate. Solar radiation is absorbed by plants and transformed into biomass (chemical exergy) at a rate of 37 TW, a large amount relative to the total exergy used by humans, which is estimated to be 13–14 TW (Barber, 2009; Szargut, 2005). If the photosynthetic efficiency could be improved so that autotrophs can absorb a larger portion of the total incoming solar radiation, then biomass could potentially replace all non-renewable fuels (coal, petroleum, natural gas, peat, nuclear). Therefore, it is of great importance to have a detailed understanding of the thermodynamic limits and processes of photosynthesis and ways to approach these limits.

1.1. Scope

This work bridges the gap between previous literature studies (discussed in Section 2), which only consider the physical effects of the process (evaporation and carbon dioxide sequestration) (Petela, 2008; Reis and Miguel, 2006) and those that only examine the mechanism of the photosynthetic reactions (Lems et al., 2010). Exergy balances are constructed for solar light absorption, the two photosystems, ATP synthesis, the Calvin Cycle, plant metabolism, and environmental losses (transpiration and photorespiration). These, accompanied by a glossary in Appendix B, yield clearly defined exergy efficiencies for photosynthesis understood by both thermodynamicists and biologists, thus facilitating and fostering cooperation in this important field.

The exergy analysis obviously requires the detailed description of the photosynthesis processes and reactions, which are presented in the following section.

1.2. Photosynthetic organism cell physiology and system description

Plant cells are composed of numerous organelles[2] – enclosed portions of the cellular medium (or cytoplasm) with designated functions. A plant cell with the major organelles labeled is depicted in Fig. 1a. It is beyond the scope of this article to explain all of the organelles. Instead, the focus is on the chloroplast, the organelle that captures sunlight, using it to convert carbon dioxide and water to organic matter (glucose herein). In terms of the analysis herein, two systems are specified and the efficiency is analyzed for each. For the first, the system boundaries are drawn around the chloroplast organelle; whereas, the second system is the entire plant. An enlarged image of the chloroplast is shown as Fig. 1b.

The chloroplast is surrounded by two layers of membranes that isolate its internal solution (the stroma) from the cell's main cytoplasm. Inside the chloroplast are numerous thylakoids, compartments that contain light-absorbing pigments. These thylakoids are stacked into columns called granum. The internal space of the thylakoids (called lumen) are approximately 3.5 pH units lower than the stroma, which plant cells use to store potential exergy in the form of a proton gradient. This potential can be converted to high-energy carrier molecules (ATP, Section 1.3) by a giant protein complex known as ATP synthase; this process is examined in more detail in Sections 3.1.3 and 4.1.3. An overall system diagram of the chloroplast is shown in Fig. 2.

As the double-sided arrows show, carbon dioxide, water, and oxygen are assumed to freely diffuse across the cellular boundaries while photosynthesis is occurring, and they are therefore in equilibrium in the compartments of the plant cell; the validity of this assumption is analyzed in the error analysis Section 5. Every chemical species discussed in this paper – besides carbon dioxide, water, and oxygen – is present in the stroma, where the majority of the chemical reactions (in the Calvin Cycle – described in Section 3.1.4) take place, with the concentrations of each species taken from the literature (Bassham and Buchanan, 1982). Exergy enters the system in the form of sunlight, which is absorbed by chlorophyll pigments. The pigments transform the sunlight's exergy into proton gradient exergy and electrical energy, which is stored in excited electrons (discussed in Section 1.3; see Fig. 3). The electrical exergy and proton exergy drive the reactions that convert carbon dioxide and water to glucose and molecular oxygen (using the Calvin Cycle). All exergy not transferred into the chemical bonds of glucose is destroyed – lost to the environment as waste heat (approximately at ambient temperature).

1.3. Photosynthesis at a glance

The overall reaction for photosynthesis (R1) and its standard Gibbs free energy change per mole of glucose, ΔG^o (Bassham and Krause, 1969; Voet et al., 2008) are:

$$6CO_2 + 6H_2O \xrightarrow[\text{light}]{} C_6H_{12}O_6 + 6O_2, \quad \Delta G^o = 2872\ \text{kJ/mol} \tag{R1}$$

Within the chloroplast, reaction R1 occurs as a series of steps decomposed into the "light" and "dark" reactions (Calvin Cycle). During the light reactions, large protein complexes (photosystem II and photosystem I) use chlorophyll pigment molecules (P680 and P700) to capture photons of light. The photons excite and displace electrons from these pigment molecules, leaving vacancies (Gust and Moore, 1985). The vacancies left by the displaced electrons are filled by splitting water, generating protons and oxygen gas, as shown in reaction R2 with the standard change in electrical potential, $\Delta\varepsilon^o$.

$$H_2O \rightarrow \tfrac{1}{2}O_2 + 2H^+ + 2e^-, \quad \Delta\varepsilon^o = 0.81\ \text{V} \tag{R2}$$

The excited, high-energy electrons proceed through a system of intermediate carriers (called the electron-transport chain or ETC) that pump protons against their gradient (into the lumen) and eventually reduce nicotinamide adenine dinucleotide phosphate ($NADP^+$), forming NADPH as shown in reaction R3. A diagram of the electron transport chain is presented as Fig. 3, with specifics discussed in Section 3.2. This diagram was created with redox half-reaction potentials from the literature (Nicholls and Ferguson, 2002; Voet et al., 2008; Walz, 1997a, b, c).

$$NADP^+ + H^+ + 2e^- \rightarrow NADPH, \quad \Delta\varepsilon^o = -0.32\ \text{V} \tag{R3}$$

The protons from water, as well as those pumped into the thylakoid membrane, flow down their concentration gradient and power ATP synthase, a proton turbine that drives the synthesis of water and adenosine triphosphate (ATP) from adenosine diphosphate (ADP) and phosphoric acid – shown as reaction R4. This is known as phosphorylation.

$$ADP + P_i \rightarrow ATP + H_2O, \quad \Delta G^o = 32.8\ \text{kJ/mol} \tag{R4}$$

where P_i is phosphoric acid (H_3PO_4). Reactions R2, R3, and R4 make up the individual light reactions; the overall light reaction is shown in reaction R5 (Lehninger, 1971):

$$12NADP^+ + 18ADP + 18P_i + 48\ \text{photons} \rightarrow 12NADPH + 12H^+ + 18ATP + 6H_2O + 6O_2 \tag{R5}$$

During the dark reactions (or Calvin Cycle), the ATP and NADPH produced during the light reactions are consumed to convert inorganic carbon (carbon dioxide from the air) to organic carbon (glucose). Initially, three molecules of carbon dioxide are reacted with ribulose-5-phosphate to produce six molecules of 3-phosphoglycerate. The six

[2] Organelle is defined in the Glossary (Appendix B) at the end of this paper, along with many other biological and chemical terms.

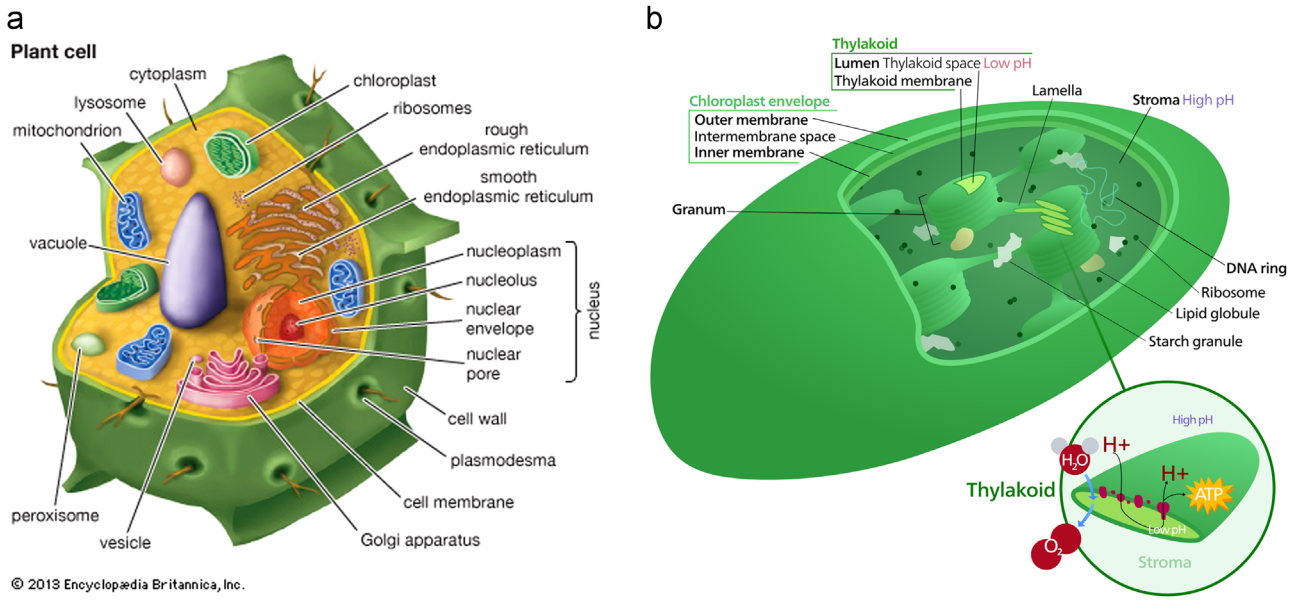

Fig. 1. (a) Plant cell with organelles labeled ((Webpage: Plant Cell Diagram; Reindl et al., 2014) By courtesy of Encyclopaedia Britannica, Inc., copyright 2013; used with permission). The nucleus is the information storage portion of the cell, where DNA is housed. In the rough endoplasmic reticulum (with ribosomes), proteins are manufactured using RNA (transcribed from DNA) as a template. The cell's fats and oils are manufactured in the smooth endoplasmic reticulum. Its' proteins are "packaged" for transport outside the cell in the Golgi apparatus. Vesicles are the packages used for transporting species to and from the cell. Vacuoles are large vesicles used for storage within the cell. Peroxisomes are chambers used for the breakdown of fats and protein components, using peroxides. Lysosomes are chambers that contain strong enzymes that can break down virtually any organic molecules. Mitochondria are used to breakdown organic sugars, like glucose, storing their chemical energy in intermediate ATP molecules. Finally, in chloroplasts (b), (Webpage: Chloroplast Diagram) photosynthesis takes place, which is the focus of this paper. Note that chloroplasts and mitochondria contain their own sets of DNA, which are used for the reproduction and maintenance of these organelles. (See the color figure in the e-copy of this manuscript.)

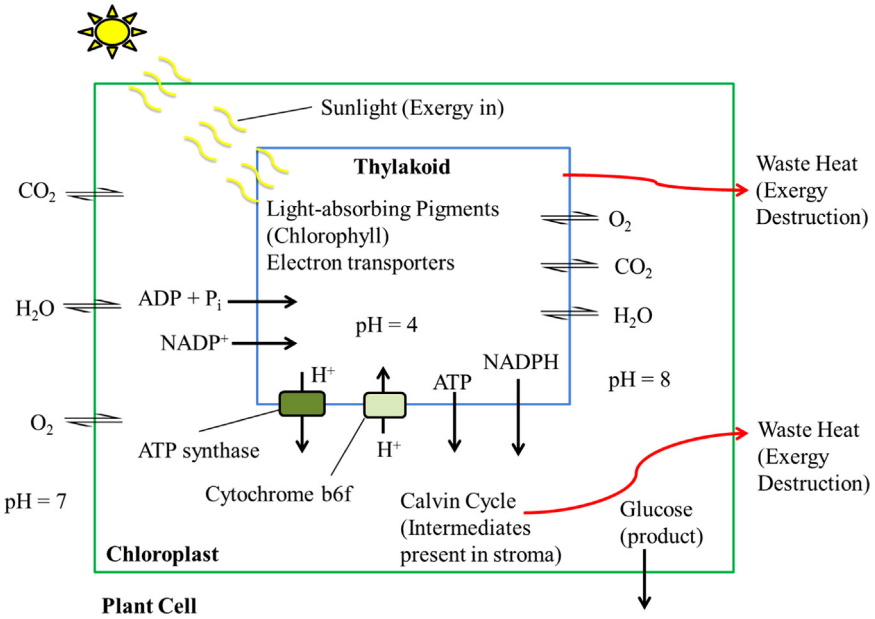

Fig. 2. Chloroplast system diagram. (See the color figure in the e-copy of this manuscript.)

molecules of 3-phosphoglycerate are reduced (using NADPH) and phosphorylated (using ATP), forming six molecules of glyceraldehyde-3-phosphate (GAl3P). One of these GAl3P molecules exits the cycle as the product. Meanwhile, the other five GAl3P molecules proceed through a series of isomerization and recombination reactions until the three molecules of ribulose-5-phosphate are regenerated. After two molecules of GAl3P have been produced, they are reacted to form glucose and phosphoric acid, the final products of photosynthesis. This series of reactions is described in more detail in Sections 3.1.4 and 4.1.4. The overall reaction is shown as reaction R6:

$$6CO_2 + 12NADPH + 12H^+ + 18ATP + 12H_2O \rightarrow C_6H_{12}O_6 + 12NADP^+ + 18ADP + 18P_i \quad \text{(R6)}$$

1.4. Definition of exergy

Exergy (B) is a thermodynamic property that expresses the maximum (reversible) mechanical work necessary to produce a

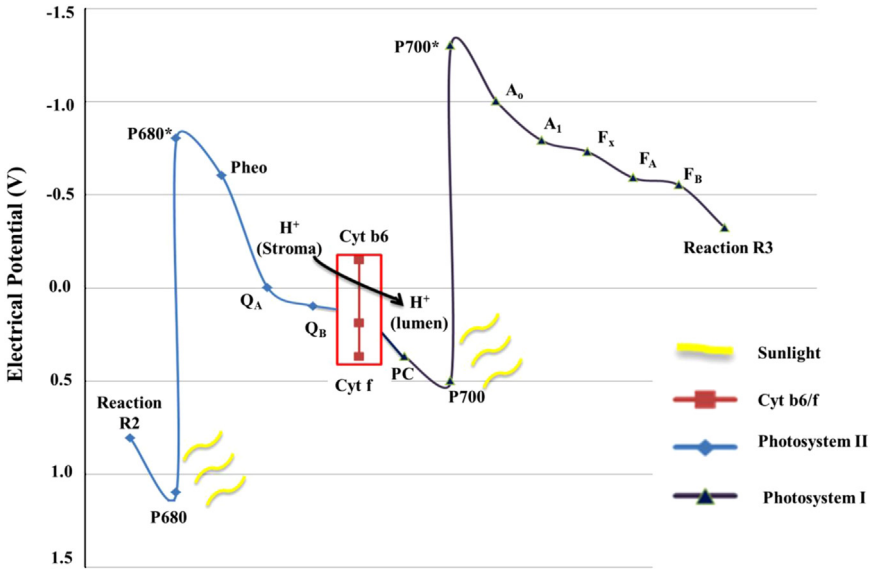

Fig. 3. Transfer of high energy electrons through photosystem II (PSII) and photosystem I (PSI) (Nicholls and Ferguson, 2002; Voet et al., 2008; Walz, 1997a, b, c). Two chemical reactions are described in this figure. The first involves splitting water into protons, oxygen, and electrons (which are then excited to a higher energy level, P680*). The second is the reduction of $NADP^+$ to NADPH using the high energy electrons and free protons. All other steps are the high-energy electrons passing through intermediate carriers, which are various functional groups in the protein complexes of PSII and PSI. (See color figure in the e-copy of this manuscript.)

material (glucose, in this case) in its specified state from components common in the natural environment (carbon dioxide and water), heat being exchanged only with the environment (Szargut, 2005). Stated differently, exergy is a measure of the quality of energy, obtained by combining the first and second laws of thermodynamics. A standard definition is shown as Eq. (1) (Keenan, 1951), where B is exergy, H is enthalpy, S is entropy, and T_o is the "dead-state" temperature (usually of the lowest relevant temperature of the surrounding environment).

$$B = H - T_o S \tag{1}$$

An exergy balance is defined based on the work of Szargut (2005), as shown in Eq. (2). Note that this formulation of the exergy balance was selected over the first principles approach (explicitly involving H and S), because this work focuses on a systems analysis of the chloroplast and not on thermodynamic derivations of properties.

$$B_{in} = B_{out,prod} + B_{out,waste} + \Delta B_{sys} + W_{sys} + \Sigma Q_{res}\left(1 - \frac{T_o}{T_H}\right) + \Sigma \delta B_i \tag{2}$$

where B_{in} is the incoming exergy of the flowing streams, $B_{out,prod}$ is the exergy leaving with the product streams, $B_{out,waste}$ is the exergy leaving with the waste streams, ΔB_{sys} is the exergy change of the system, W_{sys} is the work performed by the system, Q_{res} is the heat transferred from the system (at temperatures T_H) to a reservoir, T_o is the temperature of the "dead state", T_H is the "hot" temperature of the system, and $\Sigma \delta B_i$ is the sum of internal exergy losses (also called exergy destruction or lost work) due to irreversibilities within the system.

The "dead state" is described by the conditions (temperature, pressure, and concentration) of a system's environment at which no more useful work can be extracted from a system interacting with this environment, and it is usually closely related to the ambient conditions surrounding a system. The dead state is defined herein as at a temperature of 298.15 K, a pressure of 1 atm, and a concentration of 1 mol/L in solution (except for carbon dioxide and oxygen, whose exergies are calculated relative to their gaseous states at this temperature and pressure, and water – whose exergy is calculated relative to saturated steam at 298.15 K). These conditions were chosen to facilitate easy comparison with previous literature studies, which have used this dead state as their reference state.

Each of the exergy terms in Eq. (2) can be decomposed into the physical, chemical, electrical, and solar exergy components, as shown in Eq. (3). The meaning of each of these terms is defined in more detail in Section 3.

$$B_j = B_{phys,j} + B_{chem,j} + B_{elec,j} + B_{photon,j} \tag{3}$$

where B_j is the exergy of a particular stream or system; $B_{phys,j}$ is the physical exergy, which is due to temperature and pressure effects; $B_{chem,j}$ is the chemical exergy, which is due to chemical mixing and reactions; $B_{elec,j}$ is the exergy of electrical effects; and $B_{photon,j}$ is the exergy of sunlight.

Typically, biological systems operate at or near ambient temperatures and pressures; therefore, physical effects are small or negligible herein. For chemical exergy, the method described by Lems et al. (2007) is used. For the electrical effects, redox chemical methods are used, modified for system concentration (Lems et al., 2010; Nicholls and Ferguson, 2002). Lastly, the exergy effects of solar radiation are analyzed using the equations for photons (Lems et al., 2010; Zhu et al., 2008). The equations that describe each of these phenomena are presented in Section 3.

2. Literature review

The mechanism of photosynthesis has been known for decades, but conflicting definitions for the exergy efficiency remain, leading to efficiencies that span orders of magnitude (41% (Lems et al., 2010) to 2.6% (Petela, 2008)). Most studies that attempt to rectify this problem present yet more definitions and more variations in efficiency. The two main types of studies consider either the physical effects (evaporation, carbon dioxide sequestration, temperature changes) and ignore the complex mechanism of the photosynthetic reactions (Petela, 2008; Reis and Miguel, 2006), or the converse (Lems et al., 2010). This study incorporates both biological and mechanical effects to create a more complete picture.

The exergy property has been adopted in recent analyses of photosynthesis (Bisio and Bisio, 1998; Lems et al., 2010; Petela, 2008), but many of the earlier studies used the Gibbs free energy (defined in Eq. (4)) to calculate the "energy efficiency" (Asimov, 1968; Bassham and Buchanan, 1982; Lehninger, 1971), although enthalpy or internal energy are the appropriate variables for energy balances. Since biochemical reactions occur at approximately the ambient (or dead-state) temperature and pressure, the Gibbs free energy is essentially equal to the exergy (comparing Eq. (3) to Eq. (4)). This assumption is applied in this work solely as a means of comparison (see Section 5 for more details).

$$G = H - TS \tag{4}$$

where G is the Gibbs free energy, H is the enthalpy, S is the entropy, and T is the temperature of the system.

In principle, exergy efficiency can, and is, defined in the literature in several ways, as critically reviewed in (Lior and Zhang, 2007). Initially, the efficiency of photosynthesis was calculated by dividing the Gibbs free energy change of reaction R1 by the exergy contained in the photons (experimentally measured) (Asimov, 1968). It should be noted that these early studies used the energy values for photons; however, the exergy and energy values for photons differ only by approximately 5% (Section 3.1.1). This approach is shown as Eq. (5), and yielded exergy efficiencies between 32% and 37%.

$$\eta_{PS} = \frac{\Delta G_{rxn,R1}}{\Sigma B_{photon}} = \frac{2976}{8033} = 37\% \tag{5}$$

where η_{PS} is the exergy efficiency of photosynthesis,[3] $\Delta G_{rxn,R1}$ is the Gibbs free energy change of reaction R1, and ΣB_{photon} is the summation of the exergies for the photons required to drive reaction R1. Later studies (Albarran-Zavala and Angulo-Brown, 2007; Bassham and Buchanan, 1982; Lehninger, 1971) separated photosynthesis into the light reactions (R5) and the dark reactions (R6). The efficiencies of the light reactions were calculated using Eq. (5), replacing $\Delta G_{rxn,R1}$ with $\Delta G_{rxn,R5}$. The efficiency of the dark reactions was then calculated by comparing the Gibbs free energies of synthesizing glucose (R1) with those of NADPH and ATP, shown in Eq. (6). The total efficiency for the combined reactions was given by Eq. 7, where η_{LR} is the exergy efficiency of the light reactions and η_{CC} is the exergy of the Calvin Cycle (dark reactions, Sections 3.1.4 and 4.1.4). Efficiencies calculated using Eq. (7) are equivalent to those calculated using Eq. (5).

$$\eta_{CC} = \frac{\Delta G_{rxn,R1}}{12\Delta G_{rxn,(R2+R3)} + 18\Delta G_{rxn,R4}} \tag{6}$$

$$\eta_{PS} = \eta_{LR}\eta_{CC} \tag{7}$$

The next phenomenon, which was elucidated by experimental studies of chloroplast light absorption (Chain and Arnon, 1977), was that the photosystems (PSII and PSI) had limited ranges of absorption. In addition, models were constructed to represent the effects of light reaching the organism, and how the organism behaved with relation to the light-source and its environment (Albarran-Zavala and Angulo-Brown, 2007; Barber, 2009; Bisio and Bisio, 1998; Bolton and Hall, 1991; Petela, 2008). The standard range of absorption is known as the photo-active region (PAR), and is defined as the wavelength range from 400 nm to 700 nm (Webpage: Introduction to ozone; Bassham and Buchanan, 1982; Bolton and Hall, 1991). The relative exergy density within this region is determined using Planck's radiation distribution function (shown as Eq. (8)) and accounting for the solar spectrum at the earth's surface (Zhu et al., 2008). Note that energy density and exergy density are the same, since they are expressed on a relative basis and for sunlight the two only differ by a factor of $(1-T_{earth}/T_{sun})$. From Eq. (8), the PAR region comprises roughly 43% of the total solar exergy at the earth's surface (Webpage: Introduction to ozone; Bassham and Buchanan, 1982; Bolton and Hall, 1991), and the revised definition of photosynthetic exergy efficiency follows (Eq. (9)), yielding an efficiency of approximately 13% (Bolton and Hall, 1991).

$$SR(\lambda) = \frac{2hc^2}{\lambda^5} \times \frac{1}{e^{(hc/\lambda k_B T_s)} - 1} \tag{8}$$

$$\eta_{PS} = \eta_{PAR}\eta_{LR}\eta_{CC} \tag{9}$$

From here, there is a large divergence in the literature. Many authors calculate the photosynthetic energy and exergy efficiencies by employing heuristic estimations for the efficiencies (η) (Barber, 2009; Bugbee and Monje, 1992; Thorndike, 1996) or fractions lost (σ) (Bisio and Bisio, 1998) to the various subprocesses, as shown in Eqs. (10) and (11). These factors typically involve the light reactions, the Calvin Cycle, photorespiration (Bisio and Bisio, 1998; Kelly and Latzko, 2006c; Lems et al., 2010; Zhu et al., 2008) (Sections 3.2.3 and 4.2.3), photo-inhibition (Berry and Downton, 1982; Kelly and Latzko, 2006c), cellular metabolism (Bisio and Bisio, 1998; Zhu et al., 2008), and other stressors (most of these effects are defined in the glossary, Appendix B). Efficiencies derived from these equations are usually in the range of 2–13%, depending on the factors included.

$$\eta_{PS} = \prod_i \eta_i \tag{10}$$

$$\eta_{PS} = \prod_i (1-\sigma_i) \tag{11}$$

Three in-depth exergy studies have been conducted on photosynthesis within the last decade. The first study, by Reis and Miguel (2006), presents an exergy balance with a plant as the control volume, examining solar exergy and water fluxes throughout the system. However, the complex mechanisms occurring within the organism are ignored, and thus, the majority of the exergy lost is attributed to an "internal exergy destruction" term, which does not provide insight about how to improve the efficiency. Petela (2008) completed a similar, more complex analysis—analyzing the incoming solar radiation, the diffusive fluxes of chemical species, convective heat transfer between the leaf and the surroundings, and radiation emissions by the leaf. His calculations yield an exergy efficiency of 2.6%. However, the most substantial exergy efficiency loss (~93 percent) is due to the vaporization of liquid water, in which the plant dissipates excess heat. Thus, it provides no information on how to improve the efficiency. Lems et al. (2010) performs an exergy analysis of the light and dark reactions of photosynthesis, using photon consumption data from Voet et al. (2008). They calculate exergy efficiencies for PSII, PSI, ATP synthase, two different versions of the Calvin cycle, and the overall process (41 percent). However, the effect of poor absorbance outside the PAR and other physical phenomena are not taken into account.

Finally, Melis (2009) completes a superficial theoretical energy efficiency calculation before comparing it with experimentally measured energy efficiencies for various plants and algae. His results show that the energy efficiencies of actual organisms are 3–50 times smaller than the theoretical efficiencies due to saturation effects in photosystem II (Sections 3.1.2 and 4.1.2) and the Calvin Cycle (Sections 3.1.4 and 4.1.4).

3. Methods

The analysis in this section and Section 4 is separated into processes contained within the chloroplast and those performed

[3] Note that η is used herein to refer to exergy efficiency.

by the plant as a whole. The reason for this distinction is that chloroplasts should, in theory, perform similarly for all C3 plants. Issues concerning the overall organism (drawing water in through the roots, dealing with photorespiration, and metabolism), however, are much more dependent upon the environment, the season and time of day, and the age of the organism. In addition, this division provides guidance toward improving the efficiency using genetic modifications to adjust the chloroplast, as compared with improving the plant-based inefficiencies, which depend, for example, on the availability of water.

3.1. Chloroplast considerations

The methods for calculating the exergy required to synthesize one mole of glucose in the light and dark reactions (within the chloroplast) are presented in this section, with calculation results in Section 4.1. A qualitative exergy-flow diagram involving the four major steps of the process is shown as Fig. 4.

The physical and biological processes are subdivided as much as possible to estimate exergy flows through the latest photosynthetic mechanisms. The exergy required to drive reaction R1 is the desired output, and its ratio to the total exergy input yields the exergy efficiency. To better resolve the mechanisms, several variables are analyzed, including the exergy of photons and their imperfect absorption, the electron transport chain, the proton-motive force (PMF) and ATP synthase, and the biochemical reactions of the Calvin Cycle.

Inefficiencies due to shading and indirect sunlight are not taken into account, because these effects depend upon the organism growth location, which negatively impacts any solar radiation collector. Carbon dioxide and oxygen within the chloroplast are assumed to be in equilibrium with the surrounding environment. Water is assumed to be available in excess. This assumption is dealt with in Section 3.2.2, as drawing water from the surrounding environment is achieved by the entire organism, not the chloroplast.

3.1.1. Sunlight and absorption

Photosynthesis begins with the absorption of packets of light (photons) by light-sensitive pigments in the chloroplasts. These light-absorbing pigments are called chlorophyll, and each chlorophyll type has a different radiation absorption spectrum. All of the exergy used in photosynthesis originates from photons (except for the chemical exergy of CO_2 and water), which are collected and converted to chemical exergy during the light reactions. To determine the exergy of a mole of photons, a modified form of Planck's Law (Eq. (12)) is applied (Lems et al., 2010; Voet et al., 2008). Note that the only difference between Planck's Law and Eq. (12) is the factor $(1-(T_{earth}/T_{sun}))$, which accounts for a 5 percent difference between the energy and exergy of photons:

$$B_{photon}(\lambda) = N_A \frac{hc}{\lambda}\left(1 - \frac{T_{earth}}{T_{sun}}\right) \tag{12}$$

where B_{photon} is the photon exergy (J/mol photons) at a given wavelength (λ), N_A is Avogadro's number (6.023×10^{23}), h is Planck's constant (6.626×10^{-34} J s), c is the speed of light (3×10^8 m/s), λ is the wavelength (m), T_{earth} is the ambient temperature of the earth (298.15 K), and T_{sun} is the temperature of the sun's surface (5762 K) (Lems et al., 2010).

Photosynthetic pigments can absorb only certain ranges of wavelengths, and imperfectly at that. Plants primarily absorb sunlight in the photo-active region (PAR), which is defined to be from 400 to 700 nm (Webpage: Introduction to ozone; Bolton and Hall, 1991). A plot of the percentage of sunlight energy absorbed as a function of photon wavelength (Eq. (8)) is shown as Fig. 5 (Webpage: Introduction to ozone) Note that this is on a relative basis, so that percentages of energy and exergy absorption are the same. Factors are available for relative absorption within certain wavelength regions (Petela, 2008).

Because the calculation of photon exergy involves moles of photons, it is important to determine the average exergy for the entire mole, and to do this, the average exergy of the photon range must be taken into account. The mean-value theorem, shown as Eq. (13), is useful for finding the average of a continuous function over a well-defined interval (Webpage: Mean value theorem). More specifically, for a continuous function, $f(x)$, on a closed interval $[a, b]$, the mean-value theorem states:

$$f(c) = \frac{1}{b-a}\int_a^b f(x)dx \tag{13}$$

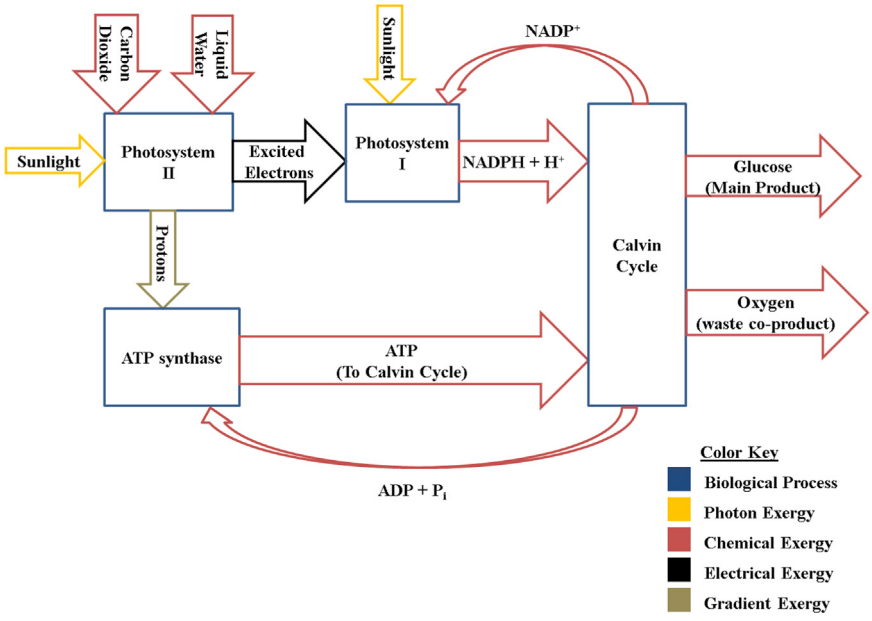

Fig. 4. Qualitative exergy-flow diagram. The color key describes the type of exergy flows between the different biological operations, as expressed in Eq. (3). (See the color figure in the e-copy of this manuscript.)

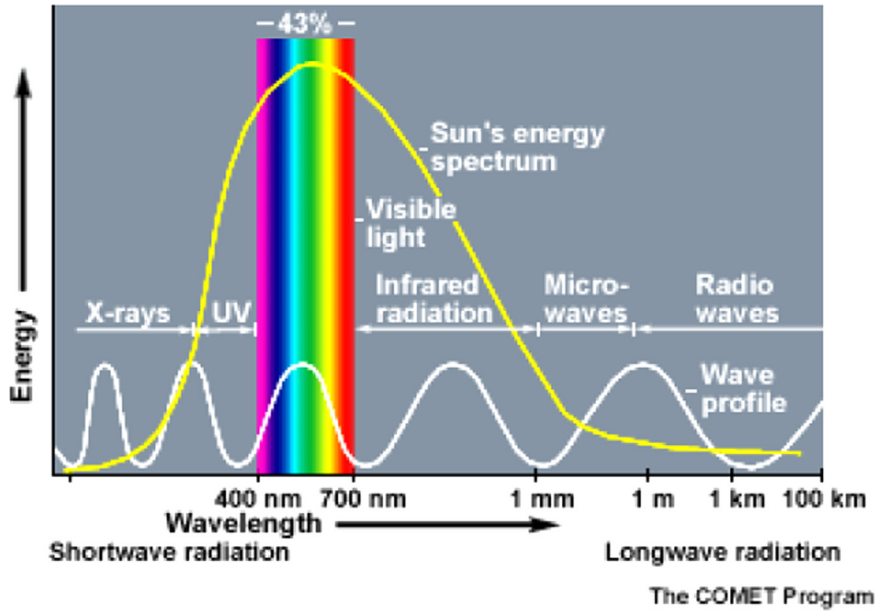

Fig. 5. Energy absorbed as a function of wavelength of sunlight ((Webpage: Introduction to Ozone), reproduced with permission from the COMET Program). The types of solar electromagnetic radiation are shown, along with their wavelengths and the relative amount of energy they represent. The region of interest for photosynthesis is 400–700 nm, the photo-active region (PAR), which represents only 43% of the total incoming energy/exergy. (See the color figure in the e-copy of this manuscript.)

where $f(c)$ is the average value of $f(x)$ on the interval $[a, b]$. Applying the mean-value theorem to Eq. (12), yields:

$$B_{\text{photon,avg}} = N_A hc\left(1 - \frac{T_{\text{earth}}}{T_{\text{sun}}}\right)\frac{\text{Ln}(\lambda_{\text{high}}) - \text{Ln}(\lambda_{\text{low}})}{\lambda_{\text{high}} - \lambda_{\text{low}}} \quad (14)$$

where $B_{\text{photon,avg}}$ is the average photon exergy (J/mol photon), N_A is Avogadro's number (6.023×10^{23}), h is Planck's constant (6.626×10^{-34} J × s), c is the speed of light (3×10^8 m/s), and λ_{high} is the maximum wavelength (m), λ_{low} is the minimum wavelength (m), T_{earth} is the ambient temperature of the earth (298.15 K), and T_{sun} is the temperature of the sun's surface (5762 K).

3.1.2. Electron transport chain

Returning to Fig. 3, photons are absorbed by the electrons within light-absorbing pigments (P680 and P700). The electrons are excited to a higher energy state, moving farther away from the pigment's core (the nuclei of a magnesium atom within a functional group called a chlorin, which is explained in the Glossary – Appendix B). Following the principle of charge-separation (Barber, 2009; Gratzel, 2001; Gust and Moore, 1985, 1989; Gust et al., 1998, 2001; Kim et al., 2012; Luo et al., 2013), the electrons are drawn away from the pigment by a series of intermediate carriers (Q_A, Q_B, PC, A_o, A_1, F_X, F_A, and F_B) forming an electron-transport chain (ETC). It is beyond the scope of this article to focus on the intermediate carriers; see references Nicholls and Ferguson (2002) and Walz (1997a, b, c) for specifics. The excited forms of both the pigments and intermediate carriers exist for only several nanoseconds (Scholes et al., 2012). In terms of exergy losses, these intermediate carriers are analogous to resistors in a wire, in that the electrons pass through, dissipating some of their potential as waste heat.

In exergy balances for carrier i (Eq. (15)), exergy that passes through an electron carrier is passed to the next carrier, used to do work within the chloroplast, or lost to the environment as low-grade, waste heat (exergy destruction):

$$B_{\text{carriers},i} = B_{\text{carriers},i-1} + W + \delta B \quad (15)$$

where $B_{\text{carrier},i}$ is the exergy of carrier i, W is the work performed by the electron transfer, and δB is the exergy destroyed. The standard reduction potentials is expressed by

$$\Delta G^\circ = -nF\Delta\varepsilon^\circ \quad (16)$$

where ΔG^o is the standard Gibbs free energy change, n is the number of moles of electrons, F is the Faraday constant (96,485 C/mol e^-), and $\Delta\varepsilon^o$ is the standard change in reduction potential. It can be modified to account for the effects of intracellular concentrations and used to calculate the exergy difference between electron carriers (Lems et al., 2010):

$$\Delta B_{\text{elec}} = B_{\text{carriers},i} - B_{\text{carriers},i-1} = nF\,\Delta\varepsilon^o + RT_o\,\text{Ln}\left(\prod [A]_i^{-\nu_i}\right) \quad (17)$$

where ΔB_{elec} is the exergy difference between carriers i and $i-1$, R is the universal gas constant (8.3143 J/mol K), T_o is the ambient temperature (298.15 K), $[A]_i$ is the activity of carrier i, and ν_i is the stoichiometric coefficient of carrier i. The changes in exergy are presented in Tables 1 and 2 in Section 4.1.2. Comparing the changes of exergy throughout the system with the amount consumed by useful work reveals the sources of exergy destruction (Eq. (15)).

3.1.3. ATP synthase

ATP synthase is an assembly of hydrophobic and hydrophilic proteins that form a transmembrane protein-complex, containing a proton-translocation channel (Voet et al., 2008). As protons flow down their concentration gradient, ATP synthase acts as a turbine, using the proton-motive force (PMF) to drive its shaft. The shaft of ATP synthase forces ADP and phosphoric acid together and supplies the necessary exergy for them to react, yielding ATP and water. ATP synthase can also function in reverse, consuming ATP to pump protons against their concentration gradient. A picture of ATP synthase is shown as Fig. 6 (Webpage: ATP synthase). Note that for chloroplasts, four protons must flow from the lumen to the stroma to produce one ATP molecule (Zhu et al., 2008).

3.1.4. Dark reactions/Calvin cycle

The Calvin Cycle is the process by which inorganic carbon (carbon dioxide from the air or bicarbonate in solution) is reduced and converted to organic sugar molecules (glucose in this analysis). Fig. 7 shows the chemical reaction mechanism as presented byBassham and Buchanan (1982), modified to include the reaction

Table 1
Exergies and reduction potentials of PSII. (See the color table in the e-copy of this manuscript.)

Photosystem II				
Electron Pair Donor	**Redox Potential, ε (V)**	**Difference $\Delta\varepsilon$ (v)**	**Standard Free Energy Change ΔG^o(J) – Eq. 16**	**Exergy Change ΔB_{elec}(J) – Eq. 17**
$2H_2O \rightarrow O_2 + 4H+$	0.81	n/a	n/a	
P680	1.10	-0.29	-671,536	-819,489
P680*	-0.80	1.90	4,399,716	4,399,716
Pheo	-0.60	-0.20	-463,128	-463,128
Qa	0.00	-0.60	-1,389,384	-1,389,384
Qb	0.10	-0.10	-231,564	-231,564
Cytochrome b6f (Cytb)	0.19	-0.09	-208,408	-208,408
Plastocyanin (PC)	0.37	-0.18	-416,815	-416,815
Total Difference PSII	**0.37**	**-0.44**	**1,018,882**	**870,928**

Note: The starting point is colored yellow, all steps that proceed naturally are green, and all steps that require an input of exergy (sunlight) are red.

Table 2
Exergies and reduction potentials of PSI. (See the color table in the e-copy of this manuscript.)

Photosystem I				
Electron Pair Donor	**Redox Potential, ε (V)**	**Difference $\Delta\varepsilon$ (v)**	**Standard Free energy Change ΔG^o(J) – Eq. 16**	**Exergy Change ΔB_{elec}(J) – Eq. 17**
Plastocyanin (PC)	0.37	n/a	n/a	
P700	0.50	0.13	-301,033	-301,033
P700*	-1.30	-1.80	4,168,152	4,168,152
A0	-1.00	0.30	-694,692	-694,692
A1	-0.79	0.21	-486,284	-486,284
Fx	-0.73	0.06	-138,938	-138,938
Fa	-0.59	0.14	-324,190	-324,190
Fb	-0.55	0.04	-92,626	-92,626
Fd	-0.53	0.02	-46,313	-46,313
NADPH	-0.32	0.21	-486,284	-486,284
Total Difference PSI	**-0.32**	**-0.69**	**1,597,792**	**1,597,792**
Total Difference (NADPH - H_2O)	**-0.32**	**-1.13**	**2,616,673**	**2,468,720**

Note: The starting point is colored yellow, all steps that proceed naturally are green, and all steps that require an input of exergy (sunlight) are red.

numbers (used in Table 3), as well as to highlight the product-producing steps (red ovals). Note that the number of lines per arrow is the number of times a reaction occurs to produce one molecule of glyceraldehyde-3-phosphate (GAl3P) – the intermediate product. Two molecules of GAl3P are consumed to produce one molecule of glucose-6-phosphate (G6P; repeating reactions C5, C6, and C7, followed by reaction C14), which is then converted to glucose by hydrolysis (not shown in Fig. 7). Finally, reactions C1–C15 are shown in Table 3; whereas, the abbreviations for the species names, and thermochemical properties of the species and reactions, are given in Appendix A, Table A.1.

The dark reactions are assumed to occur isothermally and isobarically, with exergy changes due only to chemical effects. All reaction exergy losses are released as low-grade heat (the driving force). For each molecule in the reactions, its chemical exergy is estimated using the method of Lems et al. (2007):

$$B_{\text{chem}} \approx \sum_k \left(\upsilon_k B_{\text{element},i}\right) + \Delta G_f^o + RT_o \,\text{Ln}[A] + RT_o \,\text{Ln}\left(1 + \sum_i \frac{\left(\prod_{l=1}^{i} K_l\right)}{[H^+]^i}\right) + RT_o \sum_j \text{Ln}\left(1 + \sum_i^n \left(\prod_{l=1}^{i} K_l\right)[M_j]^i\right) \quad (18)$$

where B_{chem} is the chemical exergy of a species (per mole), ν_i is the number of times that atom k occurs in the species (stoichiometric

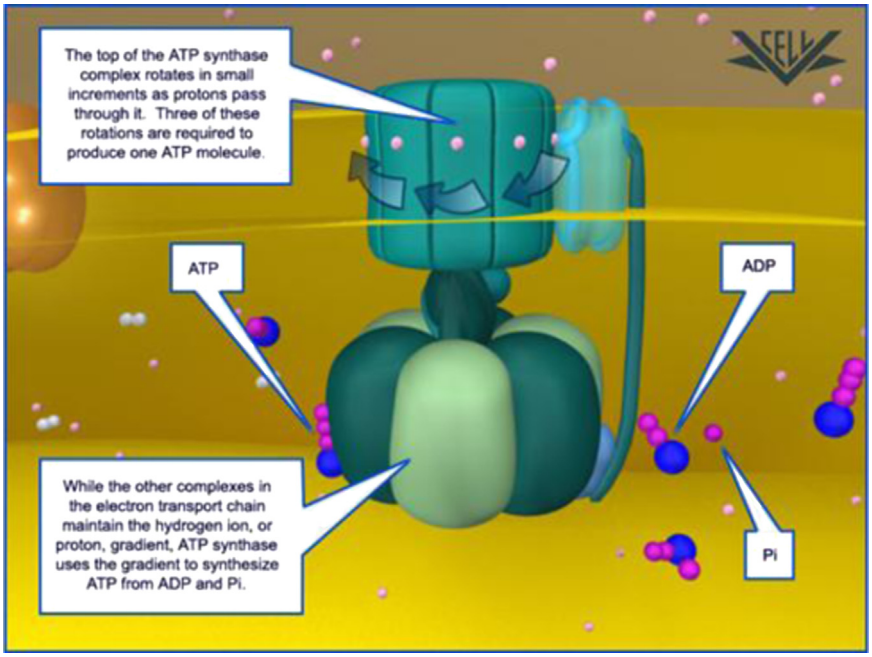

Fig. 6. Schematic of ATP synthase (Webpage: ATP synthase), reproduced with permission from NDSU VCell Animation Project). The pink spheres represent protons, the violet spheres represent phosphoric acid, and the blue spheres represent adenosine. As the protons flow down their concentration gradient (from the inside of the thylakoid, into the stroma), they turn the top of ATP synthase, as depicted by the arrows. The work from turning the top is transferred down the shaft (central or thinnest part of the protein complex), powering the lower section. The lower section uses the shaft work to force ADP and phosphoric acid to react, generating ATP and water. (See color figure in the e-copy of this manuscript.)

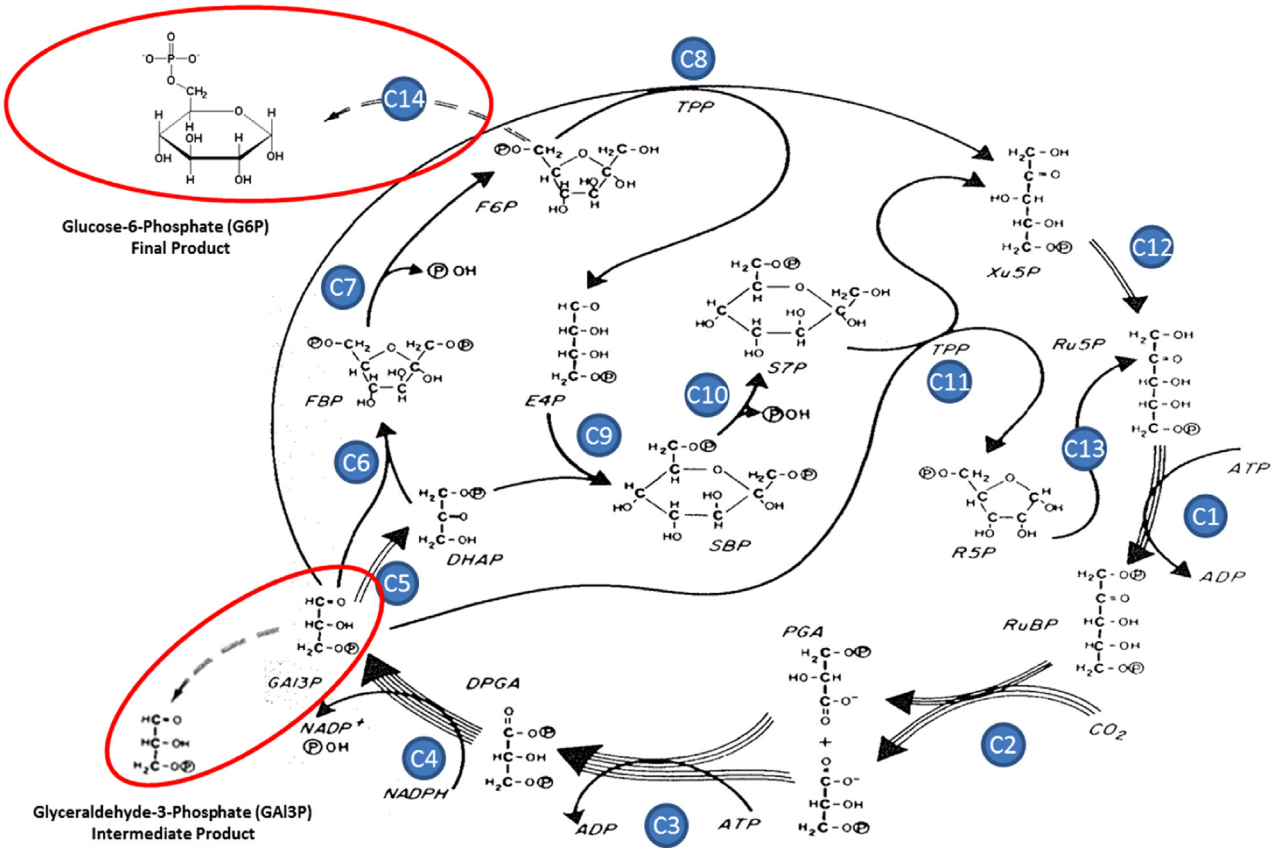

Fig. 7. The Calvin Cycle ((Bassham and Buchanan, 1982), reproduced with permission). The 14 reactions (C1–C14) shown correspond with the reaction numbers in Table 3. For every step, the number of lines that composes the arrow (for example, 6 for reaction C4) is the number of times that reaction occurs to produce one molecule of GAl3P, the intermediate product. Two molecules of GAl3P then proceed through reactions C5, C6, C7, and C14 to yield the final product G6P, which is hydrolyzed to glucose (how carbon leaves the system). In reaction C2, carbon dioxide is fixed by the enzyme RuBisCO, which is the only place carbon enters the cycle. Note that reactions C1 and C3 consume the ATP generated by ATP synthase and reaction C4 consumes the NADPH generated by PSI. (See color figure in the e-copy of this manuscript.) This article was published in Photosynthesis, Vol 2, Bassham J.A. and Buchanan B.B., Carbon Dioxide Fixation Pathways in Plants and Bacteria, page 147, Copyright Elsevier (Academic Press) (1982).

Table 3
Exergy losses in the dark reactions. (See the color table in the e-copy of this manuscript.)

Calvin Cycle				
Rxn. No.	**Reaction**	**δ*B*(J)**	**Number of Repetitions per mole of Glucose created**	**Total δ*B*(J)**
C1	(Ru5P) + (ATP) –> (RuBP) + (ADP)	16,430	6	98,582
C2	CO_2 + (RuBP) + H_2O –> 2*(PGA)	53,707	6	322,242
C3 + C4	(PGA) + (ATP) + (NADPH) –> (ADP) + (GAl3P) + ($NADP^+$) + H_3PO_4	2,729	12	32,746
C5	(GAl3P) –> (DHAP)	189	4	755
C6	(GAl3P) + (DHAP) –> (FBP)	987	2	1,974
C7	(FBP) + H_2O –> (F6P) + H_3PO_4	28,966	2	57,933
C8	(F6P) + (GAl3P) –> (E4P) + (Xu5P)	3,017	2	6,035
C9	(E4P) + (DHAP) –> (SBP)	1,011	2	2,023
C10	(SBP) + H_2O –> (S7P) + H_3PO_4	31,249	2	62,498
C11	(S7P) + (GAl3P) –> (R5P) + (Xu5P)	5,593	2	11,187
C12	(R5P) –> (Ru5P)	322	4	1,289
C13	(Xu5P) –> (Ru5P)	383	2	766
	Calvin Cycle SUM			598,030
Conversion to Glucose				
Rxn. No.	**Reaction**	**δ*B*(J)**		**Total δ*B*(J)**
C5*	(GAl3P) –> (DHAP)	189	1	189
C6*	(DHAP) + (GAl3P) –> (FBP)	987	1	987
C7*	(FBP) + H_2O –> (F6P) + H_3PO_4	28,966	1	28,966
C14	(F6P) –> (G6P)	1,298	1	1,298
C15	(G6P) + H_2O –> (Glucose) + H_3PO_4	31,768	1	31,768
	Conversion to Glucose SUM			63,208
	Total SUM			**661,239**

Note: The largest losses are shown in dark red, intermediate losses are shown as light red, then light green, and finally the smallest losses are shown as dark green.

coefficient when forming the species from reference atoms), ΔG_f^o is the standard Gibbs free energy of formation of the species, R is the universal gas constant, T_o is the dead-state temperature (298.15 K), $[A]$ is the activity of the species, K_l is the chemical equilibrium constant (for either acid, base, or metal ion dissociation) for reaction l, $[H^+]$ is the hydrogen ion concentration, $[M_j]$ is the concentration of metal ion j, k is the atom counter, i and l are the reaction counters, and j is the metal ion counter.

3.2. Plant considerations

Five issues are considered for the organism as a whole: chloroplast performance (Section 3.1), sunlight reflection by the leaves (Section 3.2.1), transpiration (Section 3.2.2), photorespiration (Section 3.2.3), and plant metabolism (Section 3.2.4). These issues were chosen because they relate directly to the organism's performance in converting sunlight, carbon dioxide, and water into biomass. Other factors, such as incident sunlight and the effects of water quality, are site dependent and thus not considered here.

3.2.1. Sunlight reflection

Some of the incident light is reflected by the surfaces of the leaves or other portions of the plant cells before the light reaches the chloroplasts. This phenomenon has been mentioned by two different authors (Bisio and Bisio, 1998; Petela, 2008); however, little discussion on the specifics was presented by either source. Again, inefficiencies due to shading and indirect sunlight are not taken into account, because these effects depend upon the organism growth location, which negatively impacts any solar radiation collector.

3.2.2. Transpiration

While plants perform photosynthesis, their pores (stomata) remain open, permitting carbon dioxide to diffuse in and oxygen to diffuse out. Water, which enters plants through their roots, is pumped into their leaves, and emitted by transpiration through their stomata. In this way, the plant cells accumulate water, which is then used by chloroplasts in Photosystem II.

Exergy losses by transpiration are estimated using Eq. (19)–(21), used by Reis and Miguel (2006). Saturated steam at T_o is the reference state for water, with liquid water at a lower exergy. Note that the chloroplasts (and leaves) are assumed to be at the environmental temperature, and carbon dioxide and oxygen are assumed to be in equilibrium with the surrounding environment. The total exergy loss is estimated by raising the water in the plant stem to height, z, and accounting for evaporation. In addition, the effect of humidity in the air must be accounted for because, for locations remote from the sea, the concentration of water vapor in the ambient air may be the most important factor in determining the chemical exergy of water; the last term in Eq. (19) accounts for this phenomena (Szargut, 2005).

$$B_w = (H - H_o) - T_o(S - S_o) + M_w g z - RT_o \,\mathrm{Ln}(\Phi_o) \tag{19}$$

$$WC = r/\phi - r \tag{20}$$

$$\delta B_{Gluc} = (WC) B_w \tag{21}$$

where B_w is the exergy of liquid water in the leaf (J/mol), T_o is the dead state temperature (298.15 K), H is the enthalpy of liquid water (J/mol), H_o is the enthalpy of saturated steam (J/mol) at T_o, S is the entropy of liquid water (J/mol-K), S_o is the entropy of saturated steam (J/mol-K) at T_o, g is the gravitational acceleration (9.81 m/s^2), M_w is the molecular weight of water (0.01802 kg/mol), Φ_o is the relative humidity, R is the universal gas constant (8.3143 J/mol-K), ϕ is the fraction of water used in photosynthesis (the remainder is lost to evaporation), r is the ratio of water to glucose in reaction R1, WC is the number of moles of water lost to evaporation without being used in the reaction, and δB_{Gluc} is the exergy destruction due to transpiration per mole of glucose produced.

3.2.3. Photorespiration

Ribulose-1,5-bisphosphate carboxylase/oxygenase (RuBisCO) is the enzyme in the Calvin Cycle that catalyzes the reaction of carbon dioxide with ribulose-1,5-bisphosphate (RuBP) in reaction C2, fixing carbon dioxide as organic carbon. About one-third to one-fourth of the time (Kelly and Latzko, 2006e), RuBisCO fixes oxygen (instead of carbon dioxide) to RuBP, forming one molecule of 3-phosphoglycerate (PGA) and one molecule of 2-phosphoglycolate (Kelly and Latzko, 2006a, c), as shown in Fig. 8 (Webpage: Photorespiration wikicommons) This is known as photorespiration (Kelly and Latzko, 2006a). The cell then initiates a series of chemical reactions, which convert the 2-phosphoglycolate to PGA and carbon dioxide (not shown in Fig. 8); the former reenters the Calvin Cycle (Kelly and Latzko, 2006a, c). Because most of these chemical reactions occur outside the chloroplast, photorespiration has been treated as associated with the entire plant. It is noteworthy, however, that the reaction that initiates this process (RuBisCO fixing oxygen) occurs exclusively inside the chloroplast.

The literature shows no concrete conclusion concerning photorespiration. In some opinions, it is considered to be an energy-dissipation mechanism to prevent photo-inhibition; that is, the oxidation of an intracellular component by excess sunlight and oxygen (Berry and Downton, 1982; Kelly and Latzko, 2006c). In other opinions, photorespiration is due to the inefficiency of RuBisCO, owing to the fact that oxygen concentrations in the air have increased drastically since RuBisCO first appeared on the Earth (Ogren, 1982). This would explain mechanisms for mitigating photorespiration, like the "C4 cycle" and crassulacean acid metabolism (Kelly and Latzko, 2006a). In either case, photorespiration is a process, which lowers the efficiency of photosynthesis.

3.2.4. Plant metabolism

Metabolism includes everything from the degradation of sugars and biomass to produce high energy molecules (like ATP) to the repair, maintenance, and manufacture of the complex proteins in the photosystems and enzymes in the Calvin Cycle. Its details are too vast to be covered in a single journal article. Simplifications are therefore made herein.

The standard reaction for cellular metabolism (called respiration) is the reverse of reaction R1 and is shown as reaction R7. Its highly spontaneous nature (due to the large chemical exergy contained within glucose) is used to drive the production of high-exergy carrier molecules, like ATP, which sustain the plant during periods of darkness. The production of ATP from glucose is shown as reaction R8 (Voet et al., 2008). Note that 38 ATP are produced in reaction R8 – the theoretical maximum. In actual practice, the number of ATP produced varies between 30 and 32, depending upon the organism that transports the molecules involved between the organelles. In addition to complete degradation, glucose can be converted to intermediates through various metabolic pathways, which build or repair organelles and other cellular components. In this way, metabolism is essentially an exergy cost for the various day-to-day intracellular operations.

$$C_6H_{12}O_6 + 6O_2 \rightarrow 6CO_2 + 6H_2O, \quad \Delta G^\circ = -2872 \text{ kJ/mol} \tag{R7}$$

$$C_6H_{12}O_6 + 6O_2 + 38ADP + 38H_3PO_4 \rightarrow 6CO_2 + 38ATP + 44H_2\,O, \quad \Delta G^\circ = -1626 \text{ kJ/mol} \tag{R8}$$

4. Analysis

The photosynthetic exergy efficiency of a terrestrial plant that has standard light absorption bands, shown in Fig. 9, is calculated in this section, using the models in Section 3. Note that the relative absorption of energy and exergy is the same (Eq. 12), and is the amount of incident solar radiation absorbed by chloroplast pigments (P680 and P700) converted to electrical work in the form of

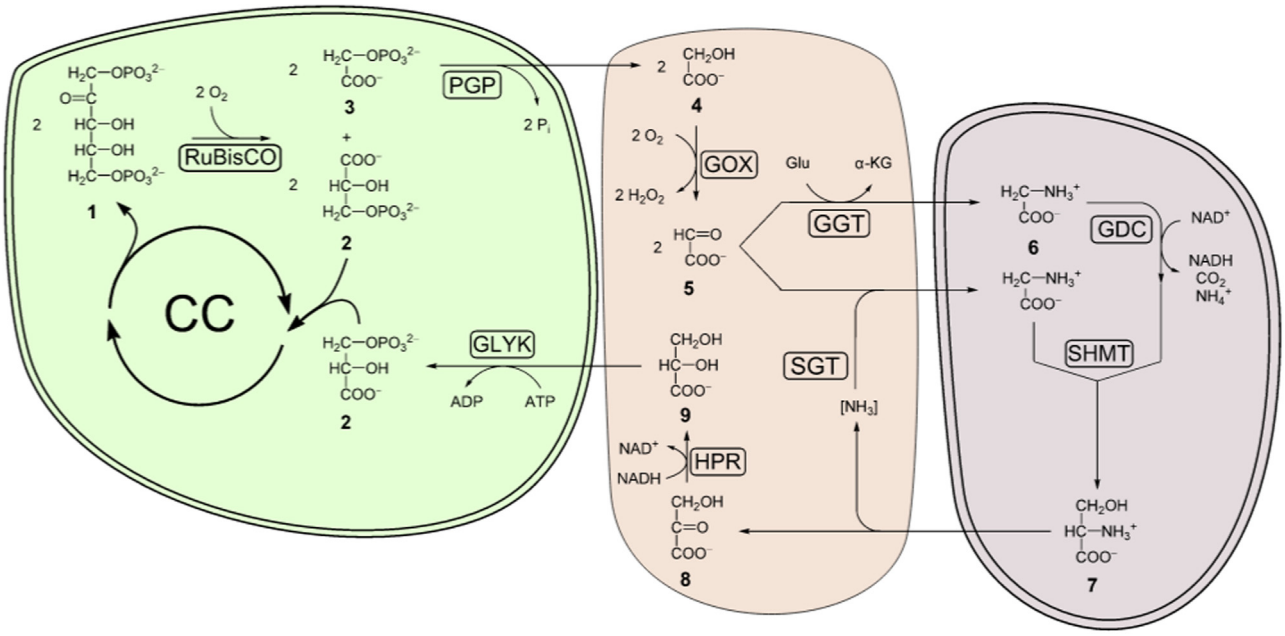

Fig. 8. Photorespiration ((Webpage: Photorespiration wikicommons) reproduced with permission). The green oval represents the chloroplast, where the Calvin Cycle (CC) takes place. RuBisCO, the enzyme responsible for fixing carbon dioxide in reaction C2 (Fig. 7), can also fix oxygen, which leads to the cycle shown here, producing 2-phosphoglycolate and 3-phosphoglycerate (molecules 3 and 2, respectively). 3-phosphoglycerate can reenter the Calvin Cycle immediately (reaction C3 in Fig. 7), but 2-phosphoglycolate must be converted to 3-phosphoglycerate before it can be returned to the Calvin Cycle. The conversion of 2-phosphoglycolate to 3-phosphoglycerate occurs between three organelles: the chloroplast, the peroxisome (shown in pink), and the mitochondria (shown in purple). (See color figure in the e-copy of this manuscript.)

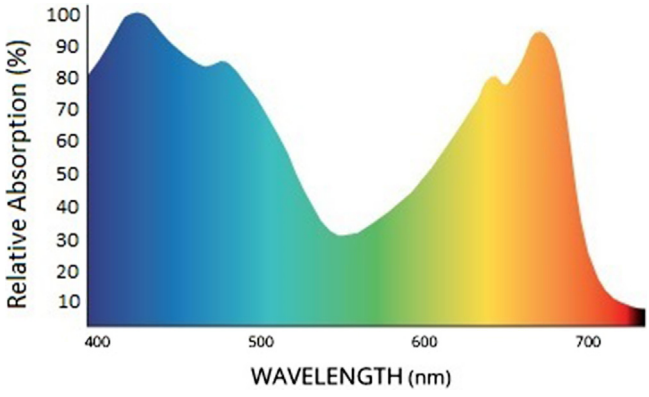

Fig. 9. Relative light absorption in the PAR (Webpage: Solar Radiation & Photosynthetically Active Radiation), reproduced with permission). Relative absorption is the amount of solar exergy absorbed by the chlorophyll pigments (P680 and P700) at a particular wavelength, relative to the total incoming solar exergy at that wavelength. (See the color figure in the e-copy of this manuscript.)

high-energy electrons. The plant's surrounding environment is temperate, with ample water, sunlight, carbon dioxide, and a relative humidity of 40 percent (arid stress conditions are not examined herein). This yields the "maximum" efficiency of photosynthesis and the causes for each exergy loss, suggesting approaches to avoid or reduce these losses.

4.1. Chloroplast efficiency

The exergy efficiency for a typical C3 chloroplast is calculated in this section and the accompanying subsections. It should be noted that this efficiency is based upon reversible exergy changes, and thus, does not account for kinetic and diffusive bottlenecks. It is representative of most C3 plant chloroplasts under non-stress conditions.

4.1.1. Sunlight and absorbance

Only a fraction of the incident solar radiation is within the PAR (Webpage: Introduction to ozone; Bolton and Hall, 1991) ($\eta_{PAR}=0.43$), the active region for chloroplast pigment absorption. It is assumed that all PAR photons that reach the chloroplast are absorbed. A small fraction of the non-PAR radiation is also absorbed, $\alpha_{non\text{-}PAR}$. Petela (2008) assigns a value of 0.05 for $\alpha_{non\text{-}PAR}$, which is used herein. Therefore, the total chloroplast exergy efficiency is

$$\eta_{solar}=\frac{B_{useful}}{B_{Total}}=\frac{\eta_{PAR}B_{sun}+\alpha_{non-PAR}(1-\eta_{PAR})B_{sun}}{B_{sun}}$$

$$=\eta_{PAR}+\alpha_{non-PAR}(1-\eta_{PAR})=0.4585 \quad (22)$$

where B_{sun} is the total incoming solar exergy (J). Note that the absorbed photons are split evenly between the two photosystems (24 photons to PSII and 24 photons to PSI).

Regarding the pigments P680 and P700, they absorb maximally (that is, the greatest amount of solar potential exergy absorbed and converted to electrical exergy) at 680 and 700 nm, respectively. The exergies of photons at these wavelengths are calculated using Eq. (12). Photons at shorter wavelengths (and, therefore, higher in exergy) are degraded to the maximal absorption wavelength (Barber, 2009). Photons at wavelenghts longer than 700 nm are instantly degraded to waste heat. When the vast majority of absorbed photons are in the PAR, it is assumed that their wavelengths are evenly distributed, with Eq. (14) determining the average exergy per mole of photons. According to Petela (2008) chloroplasts absorb marginally in the ultraviolet region, but since such a small fraction of that exergy is absorbed, it is excluded from the averaging.

The maximal wavelength, λ_{high}, is 700 nm and λ_{low} is 400 nm, yielding an average exergy of 212 kJ/(mol photon). Since P680 absorbs maximally at 680 nm, it absorbs roughly 167 kJ/(mol

photon), yielding an absorption fraction, $\eta_{PSII,abs}$:

$$\eta_{PSII,abs}=\frac{B_{useful}}{B_{Total}}=\frac{B_{PSII,maximal\ photon}}{B_{Average\ photon}}=\frac{167}{212}=0.789 \quad (23)$$

Similarly, P700 absorbs maximally at 700 nm, yielding an average exergy of 162 kJ/(mol photon) and an absorption fraction, $\eta_{PSI,abs}$:

$$\eta_{PSI,abs}=\frac{B_{useful}}{B_{Total}}=\frac{B_{PSII,maximal\ photon}}{B_{Average\ photon}}=\frac{162}{212}=0.766 \quad (24)$$

4.1.2. Electron transport chain

Reduction potentials in the electron transport chain (ETC) were taken from the literature (Nicholls and Ferguson, 2002; Voet et al., 2008; Walz, 1997a, b, c), and the change in exergy was calculated using Eqs. (17) for 24 mol of photons (n in Eq. (17) – one photon excites one electron) entering each photosystem. Note that for all pigments and intermediate electron carriers, the excited and non-excited states are assumed to have comparable activities. Consequently, when calculating the exergy changes along the electron transport chain (Fig. 3), the activity term in Eq. (17) cancels out (Bassham and Krause, 1969), and only the exergy change of the first reduction (that of P680) differs from the standard Gibbs free energy change. The validity of this assumption is examined in Section 5.

The results are shown in Table 1 for PSII and Table 2 for PSI. Cells in yellow represent the beginning state for each photosystem, cells in green represent electron transfers that proceed naturally, and cells in red represent the electron transfers that require an input of exergy (sunlight).

The only two steps in PSII that perform useful work involve the transfer of electrons from water to the pigment P680 (the first reduction) and driving protons against their gradient; that is, from Q_b to plastocyanin (PC), shown red in Fig. 3 – $Q_{pool}=\Delta B_{elec,Cytb}+\Delta B_{elec,PC}=-625{,}223$ J. In addition, exergy is delivered to PSI, shown as the "Total Difference of PSII". The work done by these processes is assumed to be 100% efficient. All exergy inputs not consumed in work-performing steps are lost as waste heat; similar to electricity flowing through a series of non-productive resistors. The incoming exergy sources to PSII are the 24 mol of photons (680 nm) and the 12 mol of water (that are split, discussed in Section 4.2.2). The exergy efficiency is

$$\eta_{PSII}=\frac{B_{useful}}{B_{Total}}=\frac{B_{water\ split}+B_{Qpool}+B_{to\ PSI}}{B_{Incoming\ Solar}+12B_w}=\frac{819{,}489+625{,}223+870{,}928}{4{,}339{,}716+30{,}520}=0.523 \quad (25)$$

Table 2 shows the exergy changes for the steps in PSI. The two inputs are the exergy from PSII and the solar exergy that further excites the electrons; whereas, the only useful work done is to reduce $NADP^+$ to NADPH, in the last step of the ETC (assumed to be completed with 100% efficiency). Again, this system is like a circuit. The intermediate molecules are similar to resistors that dissipate some of the electrical exergy. Taking the ratio of exergy consumed for useful work to total exergy input gives an efficiency of 49.0 percent:

$$\eta_{PSI}=\frac{B_{useful}}{B_{Total}}=\frac{B_{NADPH}}{B_{from\ PSII}+B_{Incoming\ Solar}}=\frac{2{,}468{,}720}{870{,}928+4{,}168{,}152}=0.490 \quad (26)$$

4.1.3. ATP synthase

From the analysis of PSII, 1,444,712 J of exergy are stored in protons within the thylakoid membrane ($B_{water\ split}+B_{Qpool}$). Calculation of the exergy of reaction R4 (Section 4.1.4 and Appendix A), gives 1,043,750 J required to create 18 mol of ATP. Note that Lems et al. (2010) assume that 24 ATP are produced. However, the correct number of ATP produced is 18 (Zhu et al., 2008), because in the chloroplast ATP synthase requires the relocation of four protons to produce one ATP. Therefore, the exergy efficiency is

$$\eta_{ATP\ synthase}=\frac{B_{useful}}{B_{Total}}=\frac{18B_{ATP}}{B_{PMF}}=\frac{1{,}043{,}750}{1{,}444{,}712}=0.722 \quad (27)$$

4.1.4. Calvin cycle/dark reactions

The stoichiometry of the overall dark reaction was presented as reaction R6, with the reactions assumed to occur at T_o and atmospheric pressure, P_o. The exergies of carbon dioxide and oxygen are calculated using Eq. (2.9) in Szargut's book (Szargut, 2005). The exergy of water (2.543 kJ/mol) is discussed in Section 4.2.2. The exergy of NADPH is calculated in Section 4.1.2; $NADP^+$ is the reference state – with exergy equal to zero. The exergies of all other chemical species, shown in Table A1, are calculated using Eq. (18), with the exergy of the chemical elements defined in Szargut's book (Szargut, 2005), the standard free energies of formation taken from Bassham and Krause (1969) and Krebs and Kornberg (1957), and the activities taken from Bassham and Krause (1969).

Only sparse data are available to estimate the acid and ion dissociation constants; therefore, the dissociation terms are neglected in this analysis. The validity of this assumption is discussed in Section 5. Also, for each compound in the dark reactions, the exergy of its elements, $B_{element}$, the Gibbs free energy of formation, ΔG_f, its activity, $[A]$, and its exergy, B_{Total}, are given in Table A1. For each reaction, it is assumed that all exergy not transferred from the reactants to the products is lost (or destroyed) as low-grade heat, which is used to evaporate water in the cell or lost as sensible heat to the environment.

As discussed in Section 1, two passes through the Calvin Cycle produce two GAl3P molecules, which are converted to glucose using a repetition of reactions, C5, C6, and C7, as well as reactions C14 and C15. The exergy losses in each reaction are shown in Table 3. Note that the reaction numbers are those in Fig. 7, and the table is color-coded, with dark red being the greatest sources of exergy destruction and dark green being the smallest. Also, "(NADPH)" and "H_3PO_4" correspond to "$NADPH+H^+$" and "P_i", respectively, in Reactions R3–R6.

From the light reactions, 3,509,191 J of exergy are transferred to the dark reactions in the form of 18 ATP and 12 NADPH. A total of 661,239 J are lost in the dark reactions, yielding the following exergy efficiency for the Calvin Cycle:

$$\eta_{Calvin\ Cycle}=\frac{B_{useful}}{B_{Total}}=\frac{18B_{ATP}+12B_{NADPH}-\delta B_{CC}}{18B_{ATP}+12B_{NADPH}}=\frac{3{,}509{,}191-661{,}239}{3{,}509{,}191}=0.812 \quad (28)$$

4.1.5. Overall chloroplast efficiency

Combining the exergy efficiencies from the previous subsections, an overall chloroplast efficiency is calculated in Table 4 and illustrated in the exergy-flow diagram in Fig. 10. In Table 4, the largest losses are shown in dark red, intermediate losses are shown as light red, then light green, and finally the smallest loss is dark green. In Fig. 10, each rectangular region represents a bioprocess whose height is proportional to its exergy flow. Exergy enters on the left, with exergy losses in the cross-hatched regions building linearly from left-to-right. Note that half of the solar exergy is transmitted to PSI, which also receives a portion of the exergy from PSII. The remainder of the solar exergy from PSII is transmitted to ATP synthase. Then, the dark reactions (Calvin Cycle) receive the NADPH exergy and the ATP exergy. One mole of glucose, the final product of photosynthesis, is then generated by the Calvin Cycle, yielding an efficiency of 12.2 percent. Note

Table 4
Overall chloroplast efficiency. (See the color table in the e-copy of this manuscript.)

Source of Exergy Destruction	Inlet (kJ)	Outlet (kJ)	Loss (kJ)	Efficiency η	Overall Loss (%)	PAR Loss (%)
PAR Reflection	9977	9977	0	1	0	0
Non-PAR Reflection	13,226	661	12,564	0.050	61.33	-
Photosystem II Absorption	5,319	4,193	1,126	0.788	5.50	14.45
Photosystem I Absorption	5,319	4,074	1,246	0.766	6.08	15.99
Photosystem II ETC	4,209	2,200	2,009	0.523	9.81	25.79
Photosystem I ETC	4,901	2,401	2,500	0.490	12.20	32.09
ATPsynthase	1,372	992	381	0.722	1.86	4.89
Calvin Cycle (Dark Reactions)	3,509	2,848	661	0.812	3.23	8.49
OVERALL	**23,334**	**2,848**	**20,487**	**0.122**	**100.0**	-

Note: The largest losses are shown in dark red, intermediate losses are shown as light red, then light green, and finally the smallest losses as dark green.

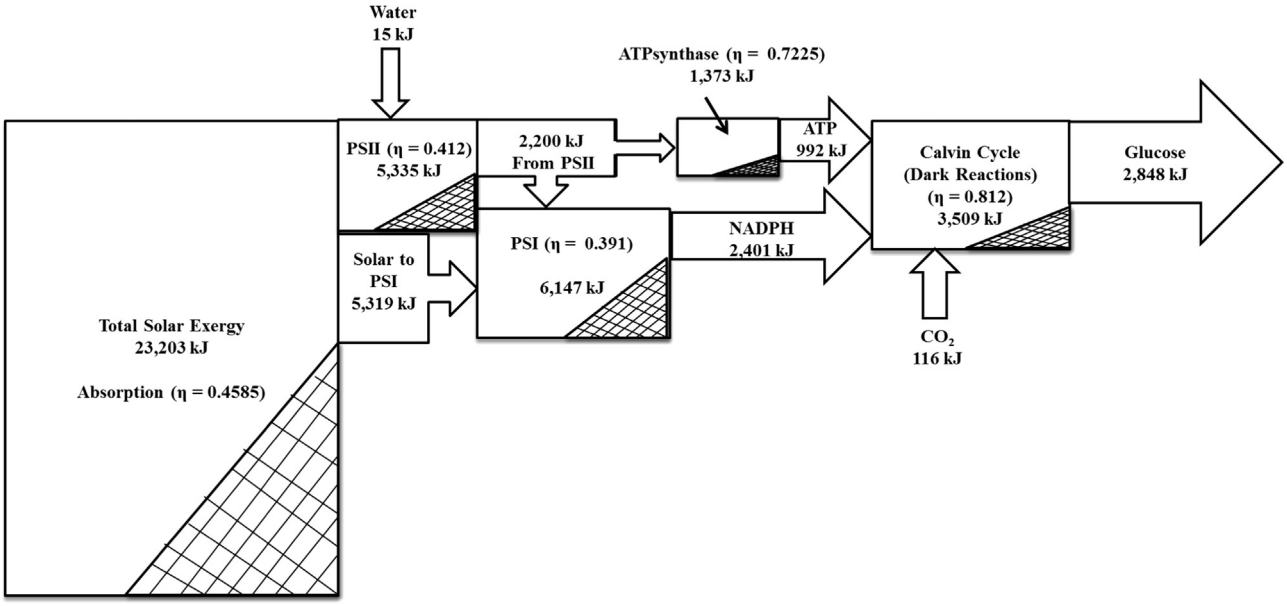

Fig. 10. Exergy-flow diagram. The exergy of the glucose product leaving the system is equal to the exergy of one mole of glucose. The 23,203 kJ of "Total Solar Exergy" was back-calculated to achieve this final value for glucose. The exergy lost by reflection or as low-grade heat is shown using the crosshatched sections.

that in Table 4, the inefficiencies due to photosystem absorption (due to the optimal absorption wavelengths) and the electron transfer chain are separated into different categories; whereas, in Fig. 10 they are lumped together inside the boxes. The impact of Table 4's results is analyzed in Section 4.2.5.

4.2. Plant efficiency

In this section, the analysis is expanded to include factors that affect the plant's efficiency, but are not contained within the chloroplast. The processes that occur within the chloroplast (Section 4.1) have a well-defined efficiency, involving clear inputs and outputs and well-defined processes. The four phenomena discussed in Section 4.2 can be thought of as sinks, which drain the plant's resources without driving the production of glucose – although some of these processes are necessary (metabolic repair and maintenance of the cellular machinery, for example).

4.2.1. Sunlight reflection

To ensure an accurate comparison between chloroplasts and other solar collectors, the reflectance of the incident solar exergy from the leaves must be taken into account (Webpage: PAR & the light spectrum). It is beyond the scope of this paper to explore the complex mechanism of leaf radiation reflection, much of which is covered by Berry and Downton (1982). Instead, a reflection factor, α_{PAR}, is used herein. The literature lists values between 0.88 and 0.80 (Bassham and Buchanan, 1982; Berry and Downton, 1982; Petela, 2008). Because the reflectance portion may be a result of light degradation by chlorophyll pigments, the higher absorption

factor ($\alpha_{PAR}=0.88$) is used herein to avoid "double-counting" exergy destruction between these two phenomena.

4.2.2. Transpiration

Returning to Section 3.2.2, transpiration is essentially water leakage from the plant's leaves, a process to minimize for optimal exergy performance. Because an efficiency does not apply, Eqs. (19)–(21) are used to determine the exergy loss to transpiration per mole of glucose produced.

Enthalpies and entropies are from the saturated steam tables at the reference state (saturated steam at T_o), and from the unsaturated water tables for the "high-exergy" state (water at T_o and P_o). For terrestrial plants, the height, z, is taken as 2.0 m. The relative humidity, Φ_o, is set at 0.4 (Petela, 2008), and the water fraction within the leaf, ϕ, is set at 0.5 (Reis and Miguel, 2006).

Eq. (19) yields the exergy of water, $B_w=2.543$ kJ/mol. The water lost by evaporation without reacting is computed using Eq. (20); that is, $WC=6/0.5-6=6$ mol of water. Using Eq. (21), the exergy destruction per mole of glucose is $\delta B_G=15{,}260$ J/(mol glucose synthesized).

It is important to note that, while the exergy loss is relatively insignificant for the temperate environment selected herein, exergy losses would be significant in an arid climate. For example, taking $\Phi_o=0.05$ and $\phi=4.31\times10^{-4}$ (Kluge, 1982) yields an exergy loss of 107,100 kJ/(mol glucose), making photosynthesis infeasible for C3 plants. In this case, plants having a cassulacean acid metabolism (CAM), a mechanism used to capture and store carbon dioxide during dark hours, are needed to conserve water (Webpage: Photorespiration wikicommons). More information about CAM is provided in the Glossary (Appendix B).

4.2.3. Photorespiration

Like transpiration, photorespiration is a process that dissipates exergy without aiding in the production of glucose. Similarly, it must be eliminated to achieve optimal photosynthesis operation. Because an efficiency does not apply, given a mechanism for photorespiration, such as that in Fig. 8, exergy losses in each reaction can be estimated using the equations in Section 3.1.4. This, however, is beyond the scope of the analysis herein.

According to Kelly and Latzko (2006a), each "CO_2 cycle" in photorespiration uses 6 NADPH and 10 ATP, yielding 1813 kJ exergy loss. Since RuBisCO has a carbon dioxide to oxygen affinity of 4:1 or 3:1, 453 kJ and 604 kJ, respectively, of photorespiration exergy losses per mole of glucose occur. Alternatively, photorespiration is known to degrade one-third to one-fourth of fixed carbon (glucose herein) (Kelly and Latzko, 2006e; Lems et al., 2010). Thus, a factor of 0.25 multiplied by the amount of fixed carbon (glucose) could be used to estimate the exergy loss, resulting in 712 kJ lost. Because the latter gives the most conservative exergy loss, it is used herein.

4.2.4. Plant metabolism

When analyzing the overall plant, plant metabolism is the most difficult to quantify. The exergy consumed by plant metabolism is higher for older plants which must maintain aged cellular components – during reproductive seasons as the plant diverts resources to producing seeds, and during the winter as less sunlight is available to provide exergy. The amount of exergy consumed is also highly dependent on the plant type (or other autotrophic organism) and the pressures associated with the surrounding environment (pests, poisons, photo-inhibition, etc.). For these reasons, the effects of metabolism must be measured experimentally on a case-by-case basis to meaningfully affect its exergy efficiency. However, two studies (Bassham and Buchanan, 1982; Bisio and Bisio, 1998) estimate one-third of fixed carbon (glucose) as the "price" for metabolism. The more precise value of 0.375 is used herein (Bisio and Bisio, 1998), which is equivalent to 1068 kJ exergy loss per mole of glucose generated.

4.2.5. Overall plant efficiency

The results of the previous subsections are tabulated as Table 5, yielding an overall plant efficiency of 3.9%, in good agreement with Petela (2008). The vast majority of the losses (greater than 87%) occur within the chloroplast (Section 4.1.5), which explains the disproportionate emphasis on the internal workings of the chloroplast herein. Table 6 is a combination of Table 4 (Section 4.1.5) and Table 5, showing the exergy losses for every step in photosynthesis. Note that "PAR Reflection" represents the leaf reflection (Section 4.2.1) and "Non-PAR Reflection" represents the rejection of non-PAR light by the chlorophyll pigments.

Clearly, the largest loss is due to the reflectance of non-PAR radiation. The second largest PAR loss (third largest loss total) is due to the degradation of photons relating to the maximal absorption wavelength of each chlorophyll pigment (P700 and P680). To improve the efficiency of photon absorption, one option is to tune the chlorophyll light-gathering antennas (Webpage: "Tuning" microalgae for high photosynthesis efficiency; Barber, 2009; Gust and Moore, 1985; Gust et al., 2001; Kelly and Latzko, 2006c; Perrine et al., 2012), which are usually composed of carotenoids that absorb light in regions of the solar spectrum where chlorophyll is ineffective. In one approach, genetic modification of the antennas are sought to harness more light to be transferred to the chlorophyll pigment, where it enters the electron transport chain (Gust and Moore, 1985). Note that genetic modifications have been reported that boost the size and effectiveness of algae antennas (Webpage:

Table 5
Overall Plant efficiency. (See the color figure in the e-copy of this manuscript.)

Source of Exergy Destruction	Inlet (kJ)	Outlet (kJ)	Loss (kJ)	Efficiency η	Overall Loss (%)
PAR Reflection	31,102	27,370	3,732	0.880	5.36
Chloroplast	68,598	7,704	60,893	0.112	87.47
Transpiration	-	-	41	-	0.06
Photorespiration	-	-	1,926	-	2.77
Plant Metabolism	-	-	2,889	-	4.15
OVERALL	**72,461**	**2,848**	**69,614**	**0.039**	**100.0**

Table 6
Overall plant efficiency with chloroplast details. (See the color table in the e-copy of this manuscript.)

Source of Exergy Destruction	Inlet (kJ)	Outlet (kJ)	Loss (kJ)	Efficiency η	Overall Loss (%)	PAR Loss (%)
PAR Reflection	31,102	27,370	3,732	0.880	5.36	14.04
Non-PAR Reflection	41,228	2,061	39,167	0.050	56.26	-
Photosystem II Absorption	14,716	11,601	3,114	0.788	4.47	11.72
Photosystem I Absorption	14,716	11,270	3,446	0.766	4.95	12.96
Photosystem II ETC	11,616	6,072	5,545	0.523	7.96	20.86
Photosystem I ETC	13,553	6,640	6,913	0.490	9.93	26.01
ATPsynthase	3,788	2,737	1,051	0.722	1.51	3.95
Calvin Cycle (Dark Reactions)	9,493	7,704	1,789	0.812	2.57	6.73
Transpiration	-	-	41	-	0.06	0.16
Photorespiration	-	-	1,926	-	2.77	7.25
Metabolism	-	-	2,889	-	4.15	10.87
OVERALL	**72,461**	**2,848**	**69,614**	**0.039**	**100.0**	**-**

"Tuning" microalgae for high photosynthesis efficiency; Perrine et al., 2012). However, the beneficial effects of increasing the antenna size have been contested (Melis, 2009). Another approach involves creating a photo-ecosystem (Bisio and Bisio, 1998), with various photosynthetic organisms having different maximal absorption wavelengths, giving maximal absorption ranges that span the entire visible spectrum (Barber, 2009). Such photo-ecosystems often have substantially higher efficiencies, as demonstrated by forests and jungles having higher biomass densities than crop fields.

Most PAR exergy losses are due to inefficiencies in PSII and PSI, during the electron transfers between carriers. Over the past 30 years, this has motivated studies (Barber, 2009; Gust and Moore, 1985) and attempts to replicate the biological electron-transport chain (ETC) (Gust and Moore, 1989; Gust et al., 1998, 2001; Kim et al., 2012). Thus far, artificial ETCs have been unstable (Barber, 2009; Kim et al., 2012). Some charge-separation is necessary to draw electrons away from the pigment molecules (Gust and Moore, 1985), and the greater the charge-separation, the more favorable the process. However, greater charge-separation yields increased exergy losses. Therefore, a method for improving photosynthetic efficiency can be found by formulating a numerical model for charge-separation, and then performing optimization (assuming that nature has not already done this) to determine the charge-separation distance for maximum efficiency. Another approach (possibly more feasible in synthetic replications) is to have the intermediate electron carriers perform work, like the Q_{pool} complex in PSII. Note also that plastiquinol diffusion within the thylakoid membrane is the rate-limiting step of the ETC (Kelly and Latzko, 2006c; Melis, 2009), which consequently is the rate-limiting step in carbon dioxide saturated photosynthesis (Kelly and Latzko, 2006b).

The next most substantial loss of PAR exergy, besides those of the photosystems, is due to the plant's metabolism, with photorespiration being of a similar order of magnitude. Some level of metabolism is essential for the plant's reproduction and maintenance of its biological machinery, and therefore the majority of these losses are likely unavoidable. In terms of photorespiration, thus far, attempts to remove it genetically have been unsuccessful (Kelly and Latzko, 2006d). But, a lower oxygen content in the local environment is most effective in decreasing losses to photorespiration. Note that aquatic organisms, such as algae, typically have almost negligible rates of photorespiration – as oxygen has a low solubility in water. In addition, algae concentrate dissolved carbon dioxide (as bicarbonate) inside their cells using pumps (Kelly and Latzko, 2006b; Ogren, 1982). This pumping is against a concentration gradient, and thus, consumes exergy, but it is a small cost compared to photorespiration.

The Calvin Cycle and ATP synthase have relatively small exergy losses, and some degree of exergy loss is required to drive the process forward at a reasonable rate. In the limit of negligible exergy loss, these processes would take an infinite amount of time, which is infeasible. Note that although not limiting in a thermodynamic sense, the Calvin Cycle can cause substantial decreases in exergy efficiency by slowing down photosynthesis (Webpage: "Tuning" microalgae for high photosynthesis efficiency; Melis, 2009). This justifies the search for genetic modifications of key enzymes (particularly SBPase (Kelly and Latzko, 2006d) and RuBisCO (Melis, 2009)) to increase the actual efficiency of photosynthesis.

Transpiration in non-arid environments causes small losses of exergy that are not worthy of further analysis. Managing transpiration in arid environments would depend largely upon irrigation techniques, which are beyond the scope of this work.

Overall, the exergy efficiency calculated herein (3.9%) is higher than that typically observed for terrestrial-plant photosynthesis (about 1%), although it is reasonable for algae (3–4%) (Bassham and Buchanan, 1982). The higher value for efficiency is because mass-transfer limitations and kinetic hold-ups were not taken into account, because only reversible transfer of exergy is modeled. As such, the efficiency computed herein is an upper bound for terrestrial plants that have not been genetically modified.

Table 7
Error analysis table.

Point of comparison	Source of comparison	Maximum percent difference
PAR reflection	Bisio and Bisio (1998)	18.6
PAR reflection	Bassham and Buchanan (1982)	5.4
Average photon exergy	Zhu et al. (2008)	8.9
Loss to reflection and re-transmittance	Bisio and Bisio (1998)	2.9
Excitation of P680	Nicholls and Ferguson (2002) and Walz (1997a, b, c)	9.0
Excitation of P700	Nicholls and Ferguson (2002) and Walz (1997a, b, c)	7.0
Redox potential of ETC (per step)	Lems et al. (2010)	1.0
Exergy of NADPH	Lems et al. (2010)	3.0
PMF exergy	Lems et al. (2010)	4.4
ATP hydrolysis	Lems et al. (2010)	12.0
Overall light reaction efficiency	Bassham and Buchanan (1982)	0.0
Overall light reaction efficiency	Lems et al. (2010)	32.0[a]
ATP synthase efficiency	Lems et al. (2010)	17.1
Calvin cycle efficiency	Bassham and Buchanan (1982) and Lems et al. (2010)	2.4
Calvin cycle efficiency	Lems et al. (2010)	4.7
Transpiration	Reis and Miguel (2006)	900.0[b]
Photorespiration	Bolton and Hall (1991)	50.0
Photorespiration	Lems et al. (2010)	25.0
Photorespiration	Kelly and Latzko (2006a)	57.2
Overall photosynthetic efficiency	Bisio and Bisio (1998)	30.0
Overall photosynthetic efficiency	Bassham and Buchanan (1982)	95.0

[a] Ref. Lems et al. (2010) neglected reflectance and imperfect light absorption. Adjusting for this herein yields a difference of 4.3%.
[b] Transpiration was calculated differently in the two studies. Even though the values were dissimilar, transpiration had a marginal effect on the overall efficiency.

5. Error analysis and validation

All data used herein were taken from previous literature sources. It is assumed that these data are accurate. No standard deviations were reported; thus, it was impossible to analyze the errors originating from measurement inaccuracies. The comparisons discussed in this section are calculated using Eq. (29) and tabulated in Table 7.

$$\text{Maximum percent difference} = \frac{|LV - SV|}{|LV|} \tag{29}$$

where SV is the "standard value" (used herein) and LV is the literature value that is the largest deviation from SV.

Different PAR radiation percentages are reported (Bassham and Buchanan, 1982; Bisio and Bisio, 1998). The true value depends on location, time of day, time of year, and weather conditions. However, all sources report absorption fractions between 0.40 and 0.50; many agreeing on roughly 0.43.

With regard to the assumption that the excited and ground-state compounds are present in roughly equal concentrations, the appendix in Lems et al. (2010) provides a thorough calculation of the ratio of [P700]/[P700$^+$], which equals 11. This yields an exergy change proportional to $\ln([P700]/[P700^+])=2.4$. Because the exergies of the other carriers (e.g., NADPH) are on the order of 200 kJ, differences of only one percent are anticipated. However, the redox potentials in Tables 1 and 2 (Nicholls and Ferguson, 2002; Voet et al., 2008; Walz, 1997a, b, c), when compared with the incoming exergy of the photons using Eq. (12), differ by approximately nine percent for PSII and seven percent for PSI. When the factor, $(1-T_{earth}/T_{sun})$, is neglected, these differences are reduced to 4.2 and 1.6 percent. These differences are attributed to the crude calculation of activities in Eq. (17). More accurate concentration information would improve these estimates.

Comparing the exergy value of NADPH computed in Table 2 (2468 kJ) with that of Lems et al. (2010) (2541 kJ), yields approximately a 3% difference. Similarly, for the exergy transferred to the PMF from PSII, the values are 1508 kJ and 1444 kJ, yielding a 4.4% difference. In this work, the exergy change of ATP hydrolysis (R4) is 58 kJ, in contrast with the commonly accepted 50–51 kJ (13.7 percent difference). The 58 kJ value is in good agreement with Lems et al. (2007) (the source of Eq. (18)), despite neglecting the acidic and ionic dissociation effects. Clearly, the exergy calculation method needs further attention. Note that this causes a decrease in Calvin Cycle efficiency (81 percent compared with 85 percent in Lems et al. (2010), and 83 percent in Bassham and Buchanan (1982)). The ATP synthase efficiency is lower here when compared with Lems et al. (2010) (72 percent compared with 82 percent in Lems et al. (2010)), because they assume that an ATP molecule is generated for every three protons moved from the lumen to the stroma; however, most sources report that it takes four protons to generate an ATP molecule in the chloroplast (Voet et al., 2008; Zhu et al., 2008).

The overall efficiency of the light reactions, 32 percent herein, is in exact agreement with Bassham and Buchanan (1982). Lems et al. (2010) predict 47 percent, but they do not account for the imperfect absorption of the average photon. When the photon absorption efficiencies of both PSII and PSI are set to unity, the efficiency herein rises to 41 percent (again, their assumption of 3 protons per ATP leads to an artificially inflated efficiency).

Exergy loss due to water evaporation (transpiration) is not examined in most studies, although the equations are fairly standard (Szargut, 2005). The results of Reis and Miguel (2006) are most relevant, although their model is based upon fluxes throughout a 24-hr cycle. Their result is an order of magnitude smaller than 21 kJ reported herein. However, both are negligible compared to the losses in the other bioprocesses analyzed. Regarding photo-respiration, no rigorous modeling has been done. The estimates of exergy destruction are based upon two other studies (Bolton and Hall, 1991; Lems et al., 2010).

Finally, the overall exergy efficiency is comparable to flux-based studies (Petela, 2008; Reis and Miguel, 2006), even though it does not account for irreversible processes and fluxes (like carbon dioxide diffusion and ETC bottlenecks), which would need to be analyzed using irreversible thermodynamics (Kjelstrup et al., 2010; Sliepcevich and Finn, 1963). This implies that diffusive fluxes have a small impact on the overall thermodynamic efficiency (even though they may have a substantial impact on the real/observed efficiency). Non-flux based studies report higher efficiencies (Bassham and Buchanan, 1982; Bolton and Hall, 1991; Bugbee and Monje, 1992), because they do not account for photo-degradation, incomplete PAR absorption (Petela, 2008), photorespiration, or transpiration. However, when the PAR

absorption factor and absorption efficiency factors are set to unity, and losses due to transpiration and photorespiration are eliminated, the overall efficiency rises to 14 percent, in nearly perfect agreement with Chain and Arnon (1977), Bugbee and Monje (1992), and Bolton and Hall (1991).

6. Conclusions

Photosynthesis produces 100 billion tons of dry biomass annually, which is equivalent to a hundred times the weight of the human population (Barber, 2009). The biomass created on earth every second amounts to approximately 37 TJ (Szargut, 2005). In contrast, humans use only 13 TJ per second, which means that biomass theoretically has the potential to satisfy all human needs. To be realizable, however, the photosynthetic efficiency would need to be increased substantially. Almost all exergy in biomass originates as the sun's electromagnetic radiation before being converted into chemical exergy by photosynthetic organisms. Therefore, it is crucial that the mechanism and efficiencies of photosynthesis are well understood.

Prior to the analysis herein, a literature search over the last 53 years was performed, uncovering a broad array of approaches, definitions, and efficiencies. Overall, theoretical efficiency decreased with increasing knowledge of the process, decreasing from 37 percent (Asimov, 1968) to 2.61 percent (Petela, 2008). The major factors in the comprehensive analysis herein present a more thorough picture of the process and its inefficiencies.

In this study, photosynthesis is decomposed into processes that occur within the chloroplast (PAR Reflection, Non-PAR reflection, PSII Absorption, PSI Absorption, PSII ETC, PSI ETC, ATP synthase, and Calvin Cycle) and those that affect the organism as a whole (Leaf PAR Reflection, Transpiration, Photorespiration, and Plant Metabolism). The exergy changes associated with each sub-step are calculated and summed to determine the exergy efficiency of each step. These steps, in turn, are combined to yield an overall photosynthetic efficiency of 12.2% for the chloroplast and 3.9 percent for the organism as a whole.

Overall, the loss of most non-PAR radiation and the reflectance of PAR radiation account for the majority of the exergy loss (64.35 percent). Thus, it is crucial that work continue to tune the photosynthetic antennas (Webpage: "Tuning" microalgae for high photosynthesis efficiency; Melis, 2009; Perrine et al., 2012). Perhaps coupling a photosynthetic system with a photovoltaic system will prove beneficial if the photovoltaic could absorb the non-PAR radiation without the PAR radiation. Similarly, using different species of photosynthetic organisms (each of which absorbs different wavelengths) and building a photo-ecosystem (Barber, 2009; Bisio and Bisio, 1998; Scholes et al., 2012) could significantly decrease the effect of photo-degradation.

Using a controlled environment also boosts the efficiency of photosynthesis by increasing access to nutrients (water, carbon dioxide) and decreasing access to oxygen, which causes photorespiration. This is a key reason algae are promising (Sukenik et al., 1991) and have higher efficiencies (in addition to their bicarbonate pumps).

With regard to the ETC, the losses are substantial, and the attempts to improve the efficiency of this process have been mostly unsuccessful. More attention should be given to this process in future studies and research work. It is generally agreed that exergy losses to ATP synthase and the Calvin Cycle are relatively low and likely to be unavoidable. Therefore, future efforts to analyze and improve photosynthesis should focus primarily upon absorbance and the ETC.

Lastly, the major limitation herein is that losses to kinetic bottlenecks are not taken into account. For example, photosynthetic efficiencies in microalgae cultures are two to three times lower than their theoretical potential due to differences in the fast rate of light capture and the much slower downstream process of photosynthetic electron transfer and carbon fixation (Webpage: "Tuning" microalgae for high photosynthesis efficiency; Melis, 2009). This study excludes such factors because of its focus on reversible exergy transfer, which provides an upper bound. However, irreversible effects should not be ignored by those seeking to optimize the output of photosynthetic organisms.

Nomenclature

Variable, quantity, units

B	Exergy, J
W	Work, J
Q	Heat, J
T	Temperature, K
N_A	Avagadro's Number, molecules/mol
h	Planck's constant, J s
c	speed of light, m/s
λ	wavelength, nm
a	lower bounding constant, dimensionless
b	upper bounding constant, dimensionless
$f(x)$	a function, dimensionless
$f(c)$	average value of function $f(x)$, dimensionless
G	Gibbs free energy, J
F	Faraday's constant, C/mol
n	number of moles, mol
ε	redox potential, V
$[A]$	chemical activity, dimensionless
ν	stoichiometric coefficient, mol
R	ideal gas constant, J/mol-K
K	equilibrium constant, varies
$[H^+]$	concentration of protons, mol/L
$[M]$	concentration of a metal ion, mol/L
H	enthalpy, J/mol
S	entropy, J/mol-K
M_w	molecular weight, g/mol
g	gravity constant, m/s^2
z	height, m
Φ	relative humidity, dimensionless
WC	water lost to evaporation, moles of water
r	ratio of water to glucose in R1, dimensionless
ϕ	fraction of water used in photosynthesis, dimensionless
η	efficiency, dimensionless

Subscript

out	leaving the system
in	entering the system
prod	products
waste	waste
sys	internal to the system
res	reservoir (Environment)
o	ambient/dead-state
H	high
phys	physical (temperature and pressure)
chem	chemical (mixing and reactions)
elec	electrical
photon	photon (sunlight)
earth	of the earth
sun	of the sun
low	lower bound
high	upper bound

carriers refering to carriers in the ETC
element refers to chemical elements
f of formation
i series counter
j series counter
k series counter
l series counter
Gluc glucose
w water
solar relating to incoming solar exergy
useful exergy used to do work or transferred to the next process
Total total incoming exergy
PAR photo-active region
non-PAR outside of the photo-active region
PSII photosystem II
PSI photosystem I
abs absorption
water split involving the split of water in the light reactions into protons and molecular oxygen
Qpool relating to the PSII complex that pumps protons against their gradient
to PSI sent to photosystem I
Incoming Solar exergy entering the system from the sun
NADPH NADPH formation reaction (R2+R3)
from PSII Coming from photosystem II
ATP Relating to the ATP hydrolysis reaction
PMF proton-motive force
CC Calvin cycle

Greek letter

Δ change
δ destruction

Superscript

o standard and dead state for exergy

Acknowledgments

Financial support from the U.S. Department of Energy , USA for the project, Algal Biofuels (Contract DE-EE0003046), awarded to the National Alliance for Biofuels and Bioproducts (NAABB), is acknowledged gratefully. Assistance from Antonio Barberio, at the University of Pennsylvania, in formulating a quantitative model of the electron-transport chain is also gratefully appreciated.

Appendix A. Biochemical reference data

In this appendix, the thermophysical properties required to estimate the exergies of the species in the Calvin Cycle reactions (Sections 3.1.4 and 4.1.4) are discussed and tabulated in Table A1. The species are numbered in order of appearance in the Calvin Cycle reactions. Also, each molecule is abbreviated using the notation in Table 3. Note the chemical formula is that used herein; it may not represent the actual chemical formula; e.g., for NADPH/$NADP^+$ and ATP/ADP. For these pairs, an "equivalent" formula is used (Lems et al., 2007) because the excluded atoms are shared between the pairs (NADPH/$NADP^+$ and ATP/ADP) and every reaction containing ATP has ADP on the other side, and similarly with NADPH/$NADP^+$.

$B_{element}$ is the exergy of the elements, as defined by Szargut (2005) and described more thoroughly in Table A2; ΔG_f is the standard Gibbs free energy of formation for each compound, as

Table A2
Elemental exergies.

Element	Ref. species	Standard chemical exergy (species) (kJ)	Standard chemical exergy (element) (kJ/mol)
C (s,gr)	CO_2(g)	19.87	410.26
H (H_2(g))	H_2O (g)	9.49	236.09
O (O_2(g))	O_2(g)	3.97	3.97
P (s,w)	HPO_4^{-2}	–	861.4

Table A1
Calvin cycle – detailed values.

Number	Molecule	Name	Formula	$B_{elements}$ (kJ/mol)	ΔG_f (kJ/mol)	[A]	$R*T_o*Ln([A])$ (kJ/mol)	B_{total} (kJ/mol)
1	Ru5P	Ribulose 5-phosphate	$C_5H_{11}O_8P$	4227.1	−1651.1	0.000012	−28.08753085	2547.85
2	ATP	Adenosine triphosphate	$P_3O_9H_4$	3074.2	−2672.1	0.0018432	−15.6078331	386.54
3	RuBP	Ribulose 1,5-bisphosphate	$C_5H_{12}O_{11}P_2$	5212.5	−2551.5	0.00204	−15.35635622	2645.62
4	ADP	Adenosine diphosphate	$P_2O_6H_3$	2088.8	−1794.5	0.00013924	−22.01100114	272.33
5	CO_2	Carbon dioxide	CO_2	414.2	−394.4	–	–	19.40
6	H_2O	Water (liquid)	H_2O	238.1	−237.2	–	–	2.54
7	PGA	3-Phosphoglycerate	$C_3H_7O_7P$	2932.4	−1609.2	0.0014	−16.28960969	1306.93
8	NADPH	Nicotinamide adenine dinucleotide phosphate (reduced)	$H:^-+H^+$	236.1	−17.1	0.001	−17.12369359	206.01
9	GAl3P	Glyceraldehyde 3-phosphate	$C_3H_7O_6P$	2930.4	−1339.1	0.000032	−25.65614483	1565.66
10	$NADP^+$	Nicotinamide adenine dinucleotide phosphate (oxidized)	–	–	0.0	0.001	−17.12369359	0.00
11	H_3PO_4	Phosphoric acid	H_3PO_4	1223.5	−1147.6	0.001	−17.12369359	58.76
12	DHAP	Dihydroxyacetone phosphate	$C_3H_7O_6P$	2930.4	−1346.7	0.00064	−18.2299985	1565.47
13	FBP	Fructose 1,6-bisphosphate	$C_6H_{14}O_{12}P_2$	5860.8	−2707.8	0.000097	−22.90709704	3130.14
14	F6P	Fructose 6-phosphate	$C_6H_{13}O_9P$	4875.4	−1811.8	0.00053	−18.69749876	3044.95
15	E4P	Eryhtrose 4-phosphate	$C_4H_9O_7P$	3578.7	−1492.6	0.00002	−26.82124084	2059.36
16	Xu5P	Xylulose 5-phosphate	$C_5H_{11}O_8P$	4227.1	−1652.1	0.000021	−26.70029449	2548.24
17	SBP	Sedoheptulose 1,7-bisphosphate	$C_7H_{16}O_{13}P_2$	6509.1	−2862.8	0.000114	−22.50678437	3623.81
18	S7P	Sedoheptulose 7-phosphate	$C_7H_{15}O_{10}P$	5523.7	−1966.8	0.000248	−20.58010154	3536.35
19	R5P	Ribose 5-phosphate	$C_5H_{11}O_8P$	4227.1	−1653.4	0.000034	−25.50586194	2548.17
20	G6P	Glucose 6-phosphate	$C_6H_{13}O_9P$	4875.4	−1813.9	0.00073	−17.90383274	3043.66
21	Glucose	Glucose	$C_6H_{12}O_6$	3890.0	−917.2	0.001	−17.12369359	2955.67
*	Oxygen	Oxygen	O_2	3.97	0	–	–	3.97
*	Hydrogen	Hydrogen	H_2	–	–	–	–	236.09

Table A3
Exergy and standard Gibbs free energy changes for important reactions.

rxn1: $(NADPH)+1/2O_2 \rightarrow (NADP^+)+H_2O$
$\Delta G^o = -220.05$ kJ/mol
$\Delta B = 205.45$ kJ/mol

rxn2: $(ATP)+H_2O \rightarrow (ADP)+H_3PO_4$
$\Delta G^o = -32.8$ kJ/mol
$\Delta B = 58.0$ kJ/mol

rxn3: $C_6H_{12}O_6+6O_2 \rightarrow 6H_2O+6CO_2$
$\Delta G^o = -2872.23$ kJ/mol
$\Delta B = 2847.83$ kJ/mol

rxn4: $C_6H_{12}O_6+6(ATP)+6O_2 \rightarrow 6CO_2+6(ADP)+6H_3PO_4$
$\Delta G^o = -3069.03$ kJ/mol
$\Delta B = 3195.75$ kJ/mol

described in the literature (Bassham and Krause, 1969; Krebs and Kornberg, 1957); it should be noted that the value for phosphoric acid (which was missing from Bassham and Krause (1969)) is taken from Lems et al. (2007); $[A]$ is the activity of the species, taken from the literature (Bassham and Krause, 1969); RT Ln($[A]$) is the exergy change due to mixing; and B_{total} is the exergy of the molecule, calculated using Eq. (18). The exergy changes and standard Gibbs free energy changes for important reactions (not in the Calvin Cycle) are shown in Table A3.

Note that in Table A1, NADPH and $NADP^+$ are assumed to be present in the concentration ratio, 1:1. Also, $NADP^+$ is assumed to be the ground state, and therefore, its exergy is zero. The values for the concentrations of ATP and ADP presented by Lems et al. (2007) do not agree with those presented by Bassham and Krause (1969). The former are more recent and are used herein. Different concentration values are tabulated for both glucose and glucose-6-phosphate, all of which are within an order of magnitude, resulting in differences of less than 1% in the overall Calvin Cycle calculations. Finally, as mentioned in Section 4.1.4, the exergies for CO_2 and O_2 are calculated using Eq. (2.9) in Szargut's book (Szargut, 2005).

Appendix B. Glossary

1. ATP synthase – a giant protein complex that uses the exergy stored in proton gradients to drive ATP synthesis, as seen in reaction R4.
2. Autotroph – an organism that uses radiant or inorganic sources of exergy to produce cellular components, sugars, and high exergy carrier molecules (like ATP). Plants and algae are two examples of autotrophs.
3. C4 Cycle – a carbon fixation pathway, which lowers RuBisCO's tendency to fix oxygen and begin photorespiration. It is named for the 4-carbon molecule (oxaloacetate) which results from the first step of carbon fixation, in contrast to the 3-carbon molecule (3-phosphoglycerate) that is produced by C3 (normal) plants.
4. Chlorin – a large aromatic ring composed of carbon, nitrogen, and hydrogen. It is the central group of a chlorophyll molecule, having a magnesium atom at its center. The aromatic behavior allows for easy excitation of the shared electrons by sunlight.
5. Chlorophyll – pigment molecules present within chloroplasts that are responsible for capturing sunlight and converting it to electrical energy (high-energy electrons).
6. Chloroplast – the organelle that captures sunlight, using it to convert carbon dioxide and water to organic matter (biomass) (see Fig. 1b).
7. Crassulacean acid metabolism (CAM) – a carbon fixation pathway that reduces water loss in arid conditions. CAM plants keep their pores open at night to collect CO_2 – which is fixed into malate (a 4-carbon molecule) – and closed during the day (the opposite of normal, or C3, plants) to reduce transpiration. The malate is concentrated around the enzyme RuBisCO in the cells, essentially eliminating photorespiration.
8. Cyclic-photophosphorylation – the process by which electrons are excited by PSI and passed backward to the cytochrome b6f complex (top red node in Fig. 3), driving protons against their gradient. The electrons are then returned to PSI by plastoquinol, and the protons are used by ATP synthase to produce ATP by reaction R4.
9. Electron transport chain (ETC) – a series of functional groups that capture solar exergy, as high energy electrons, and channel these electrons through a series of carriers that increase their charge separation from the original nucleus, thus making them available for other purposes.
10. Metabolism – the physical and chemical processes in an organism that produce and maintain its components as well as those processes that absorb radiant exergy or degrade substances to provide exergy.
11. Organelle – enclosed portion of the cellular medium (cytoplasm) with a designated function (see Fig. 1).
12. P680 – a chlorophyll pigment molecule, most commonly associated with Photosystem II, that has maximal absorption of sunlight with a wavelength of 680 nm.
13. P700 – a chlorophyll pigment molecule, most commonly associated with Photosystem I, that has maximal absorption of sunlight with a wavelength of 700 nm.
14. Photo-inhibition – the overexposure of chlorophyll to sunlight, which damages these pigments through oxidation.
15. Photon – a quantum of electromagnetic radiation that has zero mass and charge, and a spin of one.
16. Photosystem I (PSI) – a protein complex that captures sunlight, using it to excite electrons to a higher energy state and eventually produce NADPH from $NADP^+$, H^+, and two excited electrons. It is composed of a chlorophyll pigment molecule (typically P700) and electron transporter molecules, which are shown in Fig. 3.
17. Photosystem II (PSII) – a protein complex that captures sunlight, using it to drive protons against their gradient and split water – releasing protons, molecular oxygen, and electrons (which are excited to a higher energy state). It is composed of a chlorophyll pigment molecule (typically P680) and electron transporter molecules, which are shown in Fig. 3.
18. Plastiquinol (PQ) – the reduced form of plastoquinone. It is the last carrier molecule in the Photosystem II electron-transport chain, bringing the electrons from Photosystem II to Photosystem I.
19. Proton-motive force – the exergy stored in the proton gradient between the inside of the thylakoid (high concentration) and the chloroplast fluid (low concentration).
20. Redox potential, ε (V) – a measure of the affinity for a chemical species to acquire electrons, thereby becoming reduced. Moving from a smaller redox potential to a larger redox potential is a process that occurs naturally, requiring no input of exergy.
21. Relative absorption – the amount of solar exergy (photons) that can be absorbed and converted to chemical or electrical exergy by chlorophyll pigments.
22. Respiration – the process by which cells decompose glucose to energy-carrier molecules like ATP, or necessary intermediates used to produce cellular components.
23. RuBisCO – official name: ribulose-1,5-bisphosphate carboxylase/oxygenase, is an enzyme which catalyzes carbon (CO_2) fixation in the Calvin Cycle. It can also catalyze the reaction of oxygen with 1,5-bisphosphate, which is the first step in photorespiration.

24. Transpiration – the loss of the plant's water reserves through pores in the leaves (known as stomata).

Appendix C. Supporting information

The spreadsheets containing these tables, as well as the others used in the calculations, are available as a Supplement to this paper. Supplementary data associated with this article can be found in the online version at http://dx.doi.org/10.1016/j.ces.2015.02.011.

References

ATP synthase, Image Credit: NDSU VCell Animation Project. ⟨http://vcell.ndsu.nodak.edu/animations/etc/atpsynthase.htm⟩ (accessed 27.01.14).

Chloroplast Diagram. ⟨https://upload.wikimedia.org/wikipedia/commons/thumb/c/c5/Chloroplast_%28borderless_version%29-en.svg/701px-Chloroplast_%28borderless_version%29-en.svg.png⟩ (accessed 03.04.14).

Introduction to ozone, ⟨http://www.ucar.edu/learn/1_5_1.htm ⟩ with permission from the COMET Program. (accessed 27.01.14).

Mean value theorem, ⟨https://en.wikipedia.org/wiki/Mean_value_theorem⟩, (accessed 27.01.14).

Photorespiration wikicommons, ⟨https://commons.wikimedia.org/wiki/File:Photorespiration_de.svg⟩ (accessed 29.01.14).

Plant cell diagram. ⟨http://media-1.web.britannica.com/eb-media/04/114904-004-29F75B95.jpg⟩ (accessed 28.07.14).

"Tuning" microalgae for high photosynthesis efficiency. ⟨http://www.lanl.gov/newsroom/news-stories/2013/March/microalgae-for-high-photosynthesis-efficiency.ph⟩ (accessed 06.02.14).

Solar Radiation & Photosynthetically Active Radiation. ⟨http://www.fondriest.com/environmental-measurements/parameters/weather/photosynthetically-active-radiation⟩ (accessed 13.03.15).

Albarran-Zavala, E., Angulo-Brown, F., 2007. A simple thermodynamic analysis of photosynthesis. Entropy 9, 152–168.

Asimov, I., 1968. Photosynthesis. Basic Books Inc, London.

Barber, J., 2009. Photosynthetic energy conversion: natural and artificial. Chem. Soc. Rev. 38, 185–196.

Bassham, J.A., Buchanan, B.B., 1982. Photosynthesis. Academic Press, New York, NY.

Bassham, J.A., Krause, G.H., 1969. Free energy changes and metabolic regulation in steady-state photosynthetic carbon reduction. Biochim. Biophys. Acta 189, 207–221.

Berry, J.A., Downton, W.J.S., 1982. Photosynthesis. Academic Press, New York, NY.

Bisio, G., Bisio, A., 1998. Some thermodynamic remarks on photosynthetic energy conversion. Energy Convers. Manage 39, 741–748.

Biswas, B., Kazakoff, S.H., Jiang, Q., Samuel, S., Gresshoff, P.M., Scott, P.T., 2013. Genetic and genomic analysis of the tree legume *Pongamia pinnata* as a feedstock for biofuels. Plant Genome 6, 1–15.

Bolton, J.R., Hall, D.O., 1991. The maximum efficiency of photosynthesis. Photochem. Photobiol. 53, 545–548.

Bugbee, B., Monje, O., 1992. The limits of crop productivity: theory and validation. BioScience 42, 494–502.

Chain, R.K., Arnon, D.I., 1977. Quantum efficiency of photosynthetic energy conversion. Proc. Natl. Acad. Sci. USA 74, 3377–3381.

Dunlop, E.H., Coaldrake, A.K., Silva, C.S., Seider, W.D., 2013. An energy-limited model of algal biofuel production: towards the next generation of advanced biofuels. AIChE J. 59, 4641–4654.

Gratzel, M., 2001. Molecular photovoltaics that mimic photosynthesis. Pure Appl. Chem. 73, 459–467.

Gust, D., Moore, T.A., 1985. A synthetic system mimicking the energy transfer and charge separation of natural photosynthesis. J. Photochem. 29, 173–184.

Gust, D., Moore, T.A., 1989. Mimicking photosynthesis. Science 244, 35–41.

Gust, D., Moore, T.A., Moore, A.L., 1998. Mimicking bacterial photosynthesis. Pure Appl. Chem. 70, 2189–2200.

Gust, D., Moore, T.A., Moore, A.L., 2001. Mimicking photosynthetic solar energy transduction. Acc. Chem. Res., 34.

Keenan, J.H., 1951. Availability and irreversibility in thermodynamics. Br. J. Appl. Phys. 2, 183–192.

Kelly, G.J., Latzko, E., 2006a. Thirty years of photosynthesis,1974–2004. In: Kelly, G.J., Latzko, E. (Eds.), Control of Carbon Metabolism Through Enzyme Regulation and Membrane-Mediated Metabolite Transport. Springer, Berlin.

Kelly, G.J., Latzko, E., 2006b. Thirty years of photosynthesis, 1974–2004. In: Kelly, G.J., Latzko, E. (Eds.), Carbon Metabolism: On Land and at Sea. Springer, Berlin.

Kelly, G.J., Latzko, E., 2006c. Thirty years of photosynthesis, 1974–2004. In: Kelly, G.J., Latzko, E. (Eds.), Carbon Metabolism: The Chloroplast's Sesquicentenary, and Some Thoughts on the Limits to Plant Productivity. Springer, Berlin.

Kelly, G.J., Latzko, E., 2006d. Thirty years of photosynthesis, 1974–2004. In: Kelly, G.J., Latzko, E. (Eds.), Carbon Metabolism: Quantification and Manipulation. Springer, Berlin.

Kelly, G.J., Latzko, E., 2006e. Thirty years of photosynthesis, 1974–2004. In: Kelly, G.J., Latzko, E. (Eds.), Carbon Metabolism: The Calvin Cycle's Golden Jubilee. Springer, Berlin.

Kim, J.H., Lee, M., Lee, J.S., Park, C.B., 2012. Self-assembled light-harvesting peptide nanotubes for mimicking natural photosynthesis. Angew. Chem. Int. Ed. 51, 517–520.

Kjelstrup, S., Bedeaux, D., Johannessen, E., Gross, J., 2010. Non-Equilibrium Thermodynamics for Engineers. World Scientific, Hackensack, NJ, USA.

Kluge, M., 1982. Photosynthesis. Academic Press.

Krebs, H.A., Kornberg, H.L., 1957. Energy Transformations in Living Matter, a Survey. Springer-Verlag, Berlin, Gottingen, Heidelberg.

Lehninger, A.L., 1971. Bioenergetics, 2nd ed W. A. Benjamin Inc., Menlo Park, California.

Lems, S., Van Der Kooi, H.J., De Swaan Arons, J., 2007. Thermodynamic analysis of the living cell: design of an exergy-based method. Int. J. Exergy 4, 339–356.

Lems, S., Van Der Kooi, H.J., De Swaan Arons, J., 2010. Exergy analyses of the biochemical processes of photosynthesis. Int. J. Exergy 7, 333–351.

Lior, N., Zhang, N., 2007. Energy, exergy, and second law performance criteria. Energy 32 (4), 281–296.

Luo, Y., Lee, J.K., Zhao, H., 2013. Challenges and opportunities in synthetic biology for chemical engineers. Chem. Eng. Sci. 103, 115–119.

Melis, A., 2009. Solar energy conversion efficiencies in photosynthesis: minimizing the chlorophyll antennae to maximize efficiency. Plant Sci. 177, 272–280.

Nicholls, D.G., Ferguson, S.J., 2002. Bioenergetics, vol. 3. Academic Press, San Diego, CA.

Ogren, W.L., 1982. Photosynthesis. Academic Press, New York, NY.

Perrine, Z., Negi, S., Sayre, R.T., 2012. Optimization of photosynthetic light energy utilization by microalgae. Algal Res. 1, 134–142.

Petela, R., 2008. An approach to the exergy analysis of photosynthesis. Sol. Energy 82, 311–328.

Reis, H.A., Miguel, A.F., 2006. Analysis of the exergy balance of green leaves. Int. J. Exergy 3, 231–237.

Scholes, G.D., Mirkovic, T., Turner, D.B., Fassioli, F., Buchleitner, A., 2012. Solar light harvesting by energy transfer: from ecology to coherence. Energy Environ. Sci. 5, 9374–9393.

Reindl, K.M., White, A.R., Johnson, C., Vender, B., Slator, B.M., McClean, P., 2014. The virtual cell animation collection: tools for teaching molecular and cellular biology. PLoS Biology, in press.

Silva, C.S., Soliman, E., Cameron, G., Fabiano, L.A., Seider, W.D., Dunlop, E.H., Coaldrake, A.K., 2014. Commercial-scale biodiesel production from algae. Ind. Eng. Chem. Res. 53, 5311–5324.

Sliepcevich, C.M., Finn, D., 1963. A macroscopic approach to irreversible thermodynamics. Ind. Eng. Chem. Fundam. 2, 249.

Sukenik, A., Levy, R.S., Levy, Y., Falkowski, P.G., Dubinksy, Z., 1991. Optimizing algal biomass production in an outdoor pond: a simulation model. J. Appl. Phycol. 3, 191–201.

Szargut, J., 2005. Exergy Method, Technical, and Ecological Applications. WIT Press, Billerica, MA.

Thorndike, E.H., 1996. Energy and the Environment. Addison-Wesley, Reading, MA, USA.

Voet, D., Voet, J.G., Pratt, C.W., 2008. Fundamentals of Biochemistry, 3rd ed. John Wiley & Sons Inc., Hoboken, NJ.

Walz, D., 1997a. Bioenergetics. In: Graber, P., Milazzo, G. (Eds.), Chloroplasts. Birkhauser; Basel, Boston, Berlin, Chapter 5.

Walz, D., 1997b. Bioenergetics. In: Graber, P., Milazzo, G. (Eds.), Photosystem II and Water Oxidation in Cyanobacteria, Algae, and Higher Plants. Birkhauser; Basel, Boston, Berlin, Chapter 7.

Walz, D., 1997c. Bioenergetics. In: Graber, P., Milazzo, G. (Eds.), The Photosystem I Reaction Center in Oxygenic Photosynthesis. Birkhauser; Basel, Boston, Berlin, Chapter 8.

Zhu, X., Long, S.P., Ort, D.R., 2008. What is the maximum efficiency with which photosynthesis can convert solar energy to biomass? Curr. Opin. Biotech. 19, 153–159.